

PROGRESS IN UNDERSTANDING HEAVY FLAVOR DECAYS

JEFFREY D. RICHMAN

Department of Physics, University of California, Santa Barbara, CA 93106

I review new results on particles containing a charm or bottom quark, focusing on measurements that give insight into the dynamics of the decay process. Leptonic and semileptonic decays are the simplest modes, and they provide detailed tests of theoretical predictions based on methods such as lattice QCD, heavy quark effective theory, and QCD sum rules. Although hadronic decays are much more complicated, the factorization hypothesis makes predictions that, at least for certain processes, are in accord with measurements. I also emphasize the importance of precise measurements of branching fractions for normalizing modes, whose uncertainties propagate into many other quantities. Rare hadronic decays are now becoming accessible to several experiments, and I discuss new results and their implications. Finally, I review b -hadron lifetime measurements, which are steadily improving in precision and which indicate a significant difference between B -meson and b -baryon lifetimes.

1 Introduction

The weak decays of hadrons containing a charm (c) or bottom (b) quark provide insight into a broad range of questions in particle physics. The main issues are (1) decay dynamics, especially the effect of strong interactions on the underlying weak decay; (2) the magnitudes of Cabibbo-Kobayashi-Maskawa (CKM) matrix elements; (3) the origin of CP violation; and (4) the physics of a host of rare processes, including flavor-changing neutral current decays, which can probe physics beyond the standard model.

In this review,^a I focus primarily on measurements that help to shed light on the dynamics of heavy-flavor decays. A detailed understanding of these processes is essential for determining the magnitudes of CKM elements. The physics of heavy-flavor decays has also proved to be a fascinating subject in its own right, since new theoretical methods have been devised to exploit the large bottom and charm quark masses, leading to some remarkable predictions that can be tested by experiment.

Progressing from the simplest to the most complicated, I describe leptonic, semileptonic, and hadronic decays, including certain rare modes. The most interesting experimental results on leptonic decays are D_s^+ measurements, where leptonic decay is Cabibbo allowed and signals have been observed. Due to constraints on the length of this review, however, my discussions of semilep-

tonic and hadronic decays are restricted almost entirely to decays of bottom mesons, omitting the vast amount of important work on charm hadrons and bottom baryons. The exceptions are the decays $D^0 \rightarrow K^- \pi^+$ and $D_s^+ \rightarrow \phi \pi^+$, which I include because of their crucial role as normalizing modes in both charm and bottom physics. From the perspective of dynamics, semileptonic B decays are especially interesting. Here, strong interaction effects are quite important, but they are sufficiently simple in many cases to allow detailed theoretical predictions that can be tested experimentally. Hadronic modes are the most difficult to describe, since strong interactions affect both currents, and final-state interactions can also come into play. However, factorization has proved to be a useful simplifying framework, at least in certain $b \rightarrow c$ decays with large energy release, and I review some of the measurements that test this idea. I also summarize new results on hadronic rare decays and discuss the question of penguin contributions to final states that are eigenstates of CP, which would complicate the interpretation of CP violation measurements. Finally, I review the status of b -hadron lifetime measurements, which also have important implications for our understanding of decay dynamics.

The use of semileptonic B decays and $B^0 \bar{B}^0$ oscillations to extract CKM elements is covered at this conference by Lawrence Gibbons,¹ who also discusses the important recent observations of $b \rightarrow u \ell^- \bar{\nu}$ modes by CLEO. Processes involving flavor-changing neutral currents are reviewed by Andrzej Buras.² Many of the theoretical issues related to heavy-flavor dynamics are discussed by

^aInvited talk presented at the 28th International Conference on High Energy Physics, 25–31 July 1996, Warsaw, Poland

Guido Martinelli.³ Rolf Landua⁴ discusses the spectroscopy of heavy-flavor hadrons. In addition, several recent articles review experimental^{5,6} and theoretical^{7,8,9,10} aspects of heavy-flavor physics.

2 Leptonic Decays

In the leptonic decay of a charged meson M (also of mass M) the quark and antiquark annihilate into a virtual W , which then produces a charged lepton and a neutrino. In this decay, the effect of strong interactions can be parametrized by a single “decay constant,” $f_M^2 \propto |\psi(0)|^2/M$, where $\psi(0)$ is the amplitude for the quarks to have zero separation. For a pseudoscalar meson, the only available four-vector that can appear in the hadronic current is q^μ , the four-momentum of the meson. The hadronic current is therefore given by $\langle 0 | J^\mu | M \rangle = i V_{qQ} f_M q^\mu$, where V_{qQ} is the appropriate CKM matrix element. The leptonic width is given by

$$\Gamma_{\text{leptonic}} = \frac{G_F^2}{8\pi} |V_{qQ}|^2 f_M^2 M m_\ell^2 \left(1 - \frac{m_\ell^2}{M^2}\right)^2, \quad (1)$$

where m_ℓ is the lepton mass and the factor m_ℓ^2 is a consequence of helicity suppression.

There is great interest in obtaining accurate measurements of decay constants partly because they can be compared with lattice QCD calculations,³ which are becoming more reliable. In addition, decay constants are needed to extract certain CKM matrix elements. For example, the $B^0 \bar{B}^0$ mixing rate is determined by $\Delta M \propto f_B^2 \mathcal{B}_B |V_{td}|^2$, where f_B is the B meson decay constant and \mathcal{B}_B is the bag constant.

Experimental study of leptonic decays of heavy-flavor mesons has been difficult for two reasons. First, the leptonic width is small compared to the total width (unlike the case in K^+ decays), since $f_M^2 M \rightarrow \text{constant}$ for large M , whereas the total decay rate is proportional to M^5 . Second, the presence of a neutrino in the final state makes reconstruction of the signal and rejection of background more difficult. The B^+ leptonic decay rate is CKM suppressed ($\propto |V_{ub}|^2$), putting it beyond the reach of current measurements. D_s^+ leptonic decay, however, is CKM favored ($\propto |V_{cs}|^2$), and it has been measured by several experiments.

The most recent measurement of $D_s^+ \rightarrow \mu^+ \nu_\mu$ has been reported by Fermilab E653,¹¹ in which

Table 1: Measurements of $D_s^+ \rightarrow \mu^+ \nu_\mu$. The branching fractions from WA75, CLEO, and E653 have been updated to reflect the 1996 PDG value for $B(D_s^+ \rightarrow \phi \pi^+)$. The normalization of the WA75 experiment is somewhat complicated, since the relative D^0 to D_s^+ cross section is determined by a different experiment (ACCMOR). The BES signal includes one $D_s^+ \rightarrow \tau^+ \nu_\tau$ candidate.

Expt	Norm. Mode	Events	$B(D_s \rightarrow \mu^+ \nu_\mu) / 10^{-3}$
WA75	$D^0 \rightarrow \mu^+ \nu_\mu X$	$8.5_{-3.0}^{+3.8}$	$4.1 \pm 1.6 \pm 2.2$
CLEO	$D_s \rightarrow \phi \pi^+$	47 ± 10	$6.6 \pm 1.9 \pm 1.7$
E653	$D_s \rightarrow \phi \mu^+ \nu_\mu$	23 ± 6	$3.0 \pm 1.3 \pm 0.8$
BES	absolute	3	15_{-6-2}^{+13+3}
Average			$4.6 \pm 0.8 \pm 1.2$

a 600 GeV/ c π^- beam is incident on an active emulsion target. Downstream of the target are 18 planes of silicon-strip detectors, a magnetic spectrometer, and a muon system. The signature for $D_s^+ \rightarrow \mu^+ \nu_\mu$ is a muon track with a kink and large transverse momentum, $P_{T\mu}$, with respect to the parent particle direction. Figure 1(a) shows the $P_{T\mu}$ distribution for the sample of one-prong kinks; most of the events are due to the decay $D^+ \rightarrow \bar{K}^0 \mu^+ \nu_\mu$, but there is a significant excess beyond the kinematic endpoint, which is attributed to $D_s^+ \rightarrow \mu^+ \nu_\mu$ decays. A fit to the $P_{T\mu}$ spectrum yields 23 ± 6 $D_s^+ \rightarrow \mu^+ \nu_\mu$ events. As a check, E653 studies a sample of neutral, two-prong vee events (Fig. 1(b)). This histogram shows a distribution of leptons mainly from $D^0 \rightarrow K^- \mu^+ \nu_\mu$, but there is no excess beyond the endpoint because the D^0 cannot decay leptonically.

The status of $D_s^+ \rightarrow \mu^+ \nu_\mu$ results is summarized in Table 1. In addition to the E653 measurement, there are previous results from WA75,¹² CLEO II,¹³ and BES.¹⁴ Normalization of the signal within each experiment is an important issue. As I will discuss later, the absolute scale of the D_s^+ branching fractions is not well known. I have renormalized all but the BES result (which is an absolute measurement) to the PDG 96¹⁵ value $B(D_s^+ \rightarrow \phi \pi^+) = (3.6 \pm 0.9)\%$. Using the renormalized branching fractions, I obtain the world average branching fraction $B(D_s^+ \rightarrow \mu^+ \nu_\mu) = (4.6 \pm 0.8 \pm 1.2) \times 10^{-3}$, which corresponds to the decay constant value

$$f_{D_s} = (241 \pm 21 \pm 30) \text{ MeV}, \quad (2)$$

where the first error combines the statistical and systematic uncertainties and the second error is

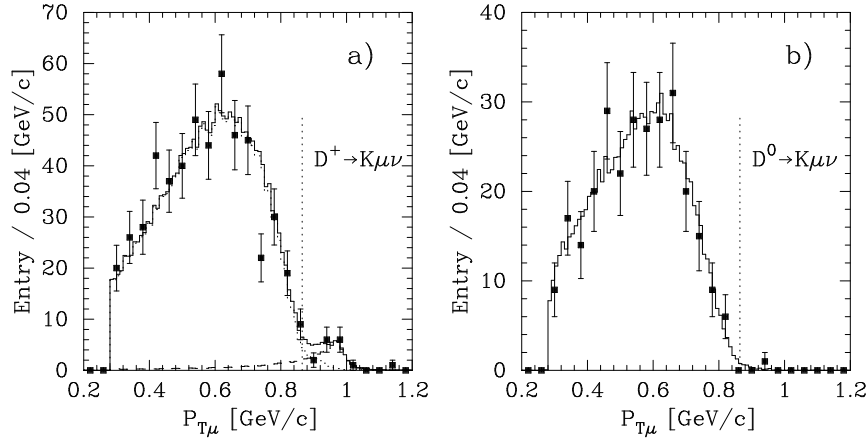


Figure 1: Observation of $D_s^+ \rightarrow \mu^+ \nu_\mu$ from E653: (a) The $P_{T\mu}$ distribution for the sample of one-prong kinks, showing the excess beyond the endpoint for the decay $D^+ \rightarrow K^0 \mu^+ \nu_\mu$ and (b) $P_{T\mu}$ distribution for the sample of two-prong vees.

due to the normalization. There are many lattice QCD calculations of f_{D_s} . A recent (preliminary) result from the MILC collaboration¹⁶ is $f_{D_s} = (211 \pm 7 \pm 25 \pm 11)$ MeV, where the last error is the estimated uncertainty due to the quenched approximation.

Also reported at this conference is a new measurement of $D_s^+ \rightarrow \tau^+ \nu_\tau$ from L3.¹⁷ In this mode, the helicity suppression is nearly absent because of the large τ -lepton mass. L3 reports a preliminary value of $B(D_s^+ \rightarrow \tau^+ \nu_\tau) = (8.9 \pm 2.6 \pm 1.1 \pm 2.1)\%$, which corresponds to $f_{D_s} = (351 \pm 53 \pm 19 \pm 37)$ MeV. Averaging this result with those from $D_s^+ \rightarrow \mu^+ \nu_\mu$ gives $f_{D_s} = (255 \pm 20 \pm 31)$ MeV.

Although data samples are much too small to observe $B^+ \rightarrow \tau^+ \nu_\tau$ at the expected branching fraction (roughly 0.5×10^{-4} to 1.0×10^{-4}), an anomalously large rate could arise as the result of physics beyond the standard model. ALEPH,¹⁸ CLEO II,¹⁹ and L3¹⁷ have obtained upper limits for this mode with a typical value of $B(B^+ \rightarrow \tau^+ \nu_\tau) < 2 \times 10^{-3}$ (90% C.L.). In the process $B^- \rightarrow \ell^- \bar{\nu}_\ell \gamma$, ($\ell = e, \mu$), the helicity suppression is removed and the branching fractions for e and μ are expected to be nearly the same, in the range 1.0×10^{-6} to 4.0×10^{-6} . These model-dependent predictions can be compared with new CLEO limits²⁰: $B(B^- \rightarrow \mu^- \bar{\nu}_\mu \gamma) < 5.2 \times 10^{-5}$ and $B(B^- \rightarrow e^- \bar{\nu}_e \gamma) < 2.0 \times 10^{-4}$ at 90% C.L.

3 Semileptonic Decays

A vast amount of information has been obtained on semileptonic decays of heavy flavors. I will begin with a simple, physical picture of semileptonic decay dynamics⁵ and then turn to measurements of exclusive decays, including detailed studies of form factors. Finally, I discuss the inclusive semileptonic branching fraction and its implications.

3.1 Dynamics of Semileptonic Decays

Semileptonic decays, because of their simplicity, provide an excellent laboratory in which to study the effect of nonperturbative QCD interactions on the weak decay process. The matrix element can be written as the product of a leptonic current, which is exactly known, and a hadronic current, which can be parametrized in terms of form factors. The form factors are Lorentz-invariant functions that may be expressed in terms of q^2 , the square of the mass of the virtual W .

Because semileptonic decays produce at least three final-state particles, q^2 is a variable that ranges from $q_{\min}^2 = m_\ell^2$ (which is nearly zero for $\ell = e$ or $\ell = \mu$) to a maximum value $q_{\max}^2 = (m_B - m_X)^2$, where X is the final-state hadron or hadronic system. The variation of the amplitude with q^2 is of great interest, since it probes the effects of strong interactions on the decay. In fact, q^2 determines the recoil velocity of the daughter

hadron in the B rest frame:

$$w = \gamma_X = \frac{E_X}{m_X} = \frac{M_B^2 + m_X^2 - q^2}{2M_B m_X}, \quad (3)$$

which also shows that by measuring E_X in the B rest frame, one can determine q^2 . This result is simply the two-body decay formula applied to a situation in which one of the particles has the variable mass $\sqrt{q^2}$.

Figure 2 shows a B meson before decay and two extreme decay configurations. At the largest value of q^2 ($w = 1$), known as the zero-recoil configuration, the full energy of the B goes into the masses of the daughter hadron and the W , as shown in Figure 2(b). The daughter hadron and the W are therefore produced at rest with respect to the B meson, and the lepton and neutrino are back to back. If both the initial and the daughter quarks are very heavy, the hadronic system is nearly undisturbed for configurations at or near q_{\max}^2 : one static source of a color field is simply replaced by another. Color magnetic moment effects, which are proportional to $1/m_Q$, are absent in this limit, so the initial and final quarks are completely equivalent. The overlap between the initial and final hadron wave functions is therefore very large, leading to a small uncertainty in the transition form factor and consequently reliable predictions for the rate as a function of $|V_{cb}|$. This ideal situation near q_{\max}^2 appears to apply reasonably well to $b \rightarrow c \ell^- \bar{\nu}$ but not to $b \rightarrow u \ell^- \bar{\nu}$ decays, where only one quark is heavy.

As q^2 decreases (and w increases), the lepton and neutrino become more collinear, and the daughter quark recoils at higher and higher velocity with respect to the spectator (Fig. 2(c)). The rapidly moving daughter quark must exchange gluons with the spectator quark in order to form a bound state. The faster the daughter quark, the more this gluon exchange suppresses the form factors, and hence the amplitude. This interaction is nonperturbative, and methods such as lattice QCD or QCD sum rules have been used to calculate the q^2 dependence of the form factors. In general, a larger range of recoil velocities leads to a larger falloff in the decay form factors. For $\bar{B} \rightarrow D^* \ell^- \bar{\nu}$ the range is a modest $\Delta w = 0.5$, whereas for $\bar{B} \rightarrow \pi \ell^- \bar{\nu}$ the range is $\Delta w = 17.9$, so the pion becomes very relativistic. Thus, $b \rightarrow c \ell^- \bar{\nu}$ decays are more tractable theoretically, both because they have a fairly reliable

normalization point at q_{\max}^2 and because the range of recoil velocities is relatively small.

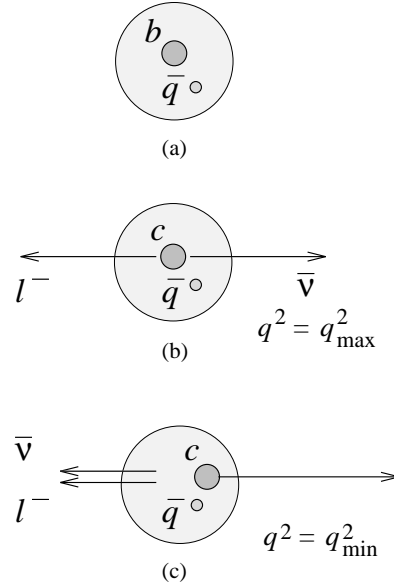


Figure 2: Kinematic configurations in semileptonic B decay (a) B meson before decay; (b) configuration at q_{\max}^2 ($w = 1$), where the daughter c quark has little velocity relative to the spectator; and (c) configuration at $q_{\min}^2 \approx 0$ ($w = w_{\max}$), where the daughter c quark has large velocity.

To understand studies of semileptonic decay dynamics, it is important to know that for a decay of the form $P \rightarrow P' \ell^- \bar{\nu}$, where both P and P' are pseudoscalar mesons, there is only one operative form factor, $F(q^2)$, assuming that the mass of the lepton is neglected. (This approximation is very good for $\ell^- = e^-$ or $\ell^- = \mu^-$.) However, for the case $P \rightarrow V \ell^- \bar{\nu}$, where V is a vector meson, the spin-polarization vector of V allows one to construct additional terms in the hadronic current, and there are three form factors, $A_1(q^2)$, $A_2(q^2)$, and $V(q^2)$, that are operative when the mass of the lepton is neglected.

Our understanding of $b \rightarrow c$ semileptonic decay has improved dramatically with the development of heavy-quark effective theory^{21,22,7} (HQET). In the heavy-quark symmetry limit ($m_b \rightarrow \infty$ and $m_c \rightarrow \infty$), all of the form factors discussed above are related to a single form factor, the Isgur-Wise function $\xi(w)$:

$$F(q^2) = \frac{(M + m_{P'})}{2\sqrt{M m_{P'}}} \xi(w)$$

$$\begin{aligned}
V(q^2) &= A_2(q^2) = \frac{A_1(q^2)}{\left[1 - \frac{q^2}{(M+m_V)^2}\right]} \\
&= \frac{(M+m_V)}{2\sqrt{Mm_V}}\xi(w). \tag{4}
\end{aligned}$$

These symmetry relations represent a major simplification, even though they do not tell us the form of $\xi(w)$. However, in the heavy-quark symmetry limit, there is one additional result, $\xi(1) = 1$, which is the form factor normalization in the zero-recoil configuration.

In the real world, of course, the quark masses are not infinite, so these results cannot be exact. The heavy-quark symmetry limit is thus only the first term in the HQET expansion in $1/m_Q$. In particular, the simple relations among the semileptonic decay form factors given above are somewhat modified.^{7,23,10} Measurements of the kinematic distributions in semileptonic decay provide an important check of these HQET-based predictions. For $b \rightarrow u\ell^-\bar{\nu}$ decays, HQET is not directly applicable, but lattice QCD calculations are beginning to produce useful predictions.

3.2 Exclusive Semileptonic B Decays

Many new results were reported at this conference on $\bar{B} \rightarrow D\ell^-\bar{\nu}$ and $\bar{B} \rightarrow D^*\ell^-\bar{\nu}$, which account for roughly two-thirds of the inclusive semileptonic rate, and on $\bar{B} \rightarrow D^{**}\ell^-\bar{\nu}$, where D^{**} indicates an orbitally excited charm meson. Improvements in $\bar{B} \rightarrow D\ell^-\bar{\nu}$ measurements have come rather slowly, partly because $\bar{B} \rightarrow D\ell^-\bar{\nu}$ has a substantial feed-down background from $\bar{B} \rightarrow D^*\ell^-\bar{\nu}$. But experimenters have also focused more on $\bar{B} \rightarrow D^*\ell^-\bar{\nu}$ because it is the preferred mode for measuring $|V_{cb}|$. In $\bar{B} \rightarrow D^*\ell^-\bar{\nu}$, there are no leading order ($1/m_Q$) power corrections to the form factor normalization at high q^2 (Luke's theorem²⁴), where the $|V_{cb}|$ measurement is performed. This result does not hold for $\bar{B} \rightarrow D\ell^-\bar{\nu}$, which has a further (but related) problem: its rate is highly suppressed at high q^2 by the kinematic factor p_D^3 , which arises from the p -wave nature of this decay. Nevertheless, it is very important for testing HQET to study the form factor shape for $\bar{B} \rightarrow D\ell^-\bar{\nu}$ and to compare it with the form factor shapes in $\bar{B} \rightarrow D^*\ell^-\bar{\nu}$. Measurements of both $\bar{B} \rightarrow D\ell^-\bar{\nu}$ and $\bar{B} \rightarrow D^*\ell^-\bar{\nu}$ also provide information that can be used to test whether factorization is a good description of the modes $\bar{B} \rightarrow D^{(*)}h$,

where h is a hadron.

Three recent measurements, two from CLEO II²⁵ and one from ALEPH²⁶, have significantly improved the situation for $\bar{B}^0 \rightarrow D^+\ell^-\bar{\nu}$. This mode typically has less background than $B^- \rightarrow D^0\ell^-\bar{\nu}$, since all D^{*0} and about 70% of D^{*+} decays produce D^0 background. One of the CLEO analyses uses a novel “neutrino reconstruction” technique, which relies on the near hermiticity of the detector. (This method was also used in the CLEO II measurements²⁷ of $\bar{B} \rightarrow \pi\ell^-\bar{\nu}$ and $\bar{B} \rightarrow \rho\ell^-\bar{\nu}$.) The four-momentum of the neutrino is determined from the missing momentum vector of the event; once this quantity is obtained, a beam-energy constrained B mass peak is reconstructed, just as for a hadronic decay analysis. Although this idea may not seem new in itself, the real advance lies in the method for obtaining good resolution on the neutrino momentum. The main idea is to restrict the sample to $B\bar{B}$ events in which there is only one semileptonic decay (by requiring no additional leptons) and no K_L 's (by requiring a small missing mass in the event). Together, these and other requirements lead to a resolution on the neutrino energy in signal events of about 110 MeV. Figure 3 shows the background-subtracted distribution of $M(D^+\ell^-\bar{\nu}_{\text{miss}})$, where ν_{miss} refers to the neutrino as reconstructed from the missing momentum vector. The signal contains 238 ± 27 events. An alternative CLEO analysis, which uses the more traditional approach of analyzing the missing mass recoiling against the $D^+\ell^-$ system, obtains a much higher yield at the expense of more background. The average of the branching fractions from these two analyses is presented in Fig. 4. The table also includes earlier results from ARGUS²⁸ and the new measurement from ALEPH²⁶, which has a signal of 266 ± 24 events. The branching fractions reported by the experiments assume D^+ branching fractions from the 1994 Particle Data Book²⁹. I have computed two averages, one from those values and a second using values updated to reflect the new $D^0 \rightarrow K^-\pi^+$ branching fraction presented in this paper.

Figure 5 shows the measured values of the quantity $F(w)V_{cb}$ as a function of w for the two CLEO analyses. The quantity $F(w)V_{cb}$ is only a part of the decay amplitude: the w dependence due to p -wave kinematics has been factored out, allowing us to see the form factor itself. It is ap-

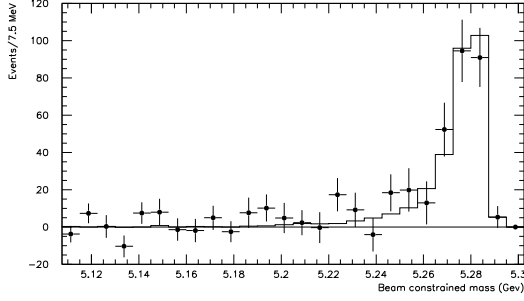


Figure 3: CLEO II measurement of $B(\bar{B}^0 \rightarrow D^+ \ell^- \bar{\nu})$ using “neutrino reconstruction.” The points with error bars are the background-subtracted distribution of $M(D\ell^- \bar{\nu})$, where the neutrino four-momentum is estimated from the missing momentum in the event.

ARGUS		$(2.0 \pm 0.7 \pm 0.6)\%$
CLEO II		$(1.78 \pm 0.20 \pm 0.24)\%$
ALEPH		$(2.41 \pm 0.21 \pm 0.44)\%$
Average		$(1.96 \pm 0.27)\%$

Figure 4: Summary of measurements of the branching fraction for $\bar{B}^0 \rightarrow D^+ \ell^- \bar{\nu}$. In the values listed, the normalization is based on the 1994 PDG value for $B(D^0 \rightarrow K^- \pi^+)$, which sets the scale for D^+ branching fractions. Updating the measurements to reflect the new value for $B(D^0 \rightarrow K^- \pi^+)$ used in this paper, one obtains $B(\bar{B}^0 \rightarrow D^+ \ell^- \bar{\nu}) = (2.03 \pm 0.28)\%$.

parent from Fig. 5 that the dependence of the form factor on w is mild, and it is well described by a linear function of slope ρ^2 . The CLEO II²⁵ measurements give $\rho^2 = 0.64 \pm 0.18 \pm 0.10$, while ALEPH²⁶ obtains $\rho^2 = 0.00 \pm 0.49 \pm 0.38$. (Both results are preliminary.) The figure also shows the linear function extracted from the CLEO $\bar{B} \rightarrow D^* \ell^- \bar{\nu}$ data, whose slope is consistent with that from $\bar{B} \rightarrow D \ell^- \bar{\nu}$. Below I will present a systematic comparison of the various measurements of the form factor slopes.

What measurements allow us to test the predictions of HQET? With data from semileptonic decay, there are essentially two approaches: (1) comparison of the different form factors governing $\bar{B} \rightarrow D^* \ell^- \bar{\nu}$ with each other and (2) comparison of $\bar{B} \rightarrow D \ell^- \bar{\nu}$ with $\bar{B} \rightarrow D^* \ell^- \bar{\nu}$. Figure 6 shows the decay angles that, together with q^2 , are used in the CLEO II measurement of the $\bar{B} \rightarrow D^* \ell^- \bar{\nu}$ form factors.^{30,31} The form factors are measured by performing a joint, four-dimensional maximum

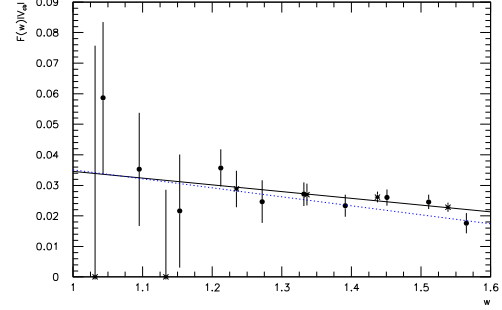


Figure 5: CLEO II measurement of the function $V_{cb} F(w)$ for $\bar{B}^0 \rightarrow D^+ \ell^- \bar{\nu}$. The points and asterisks represent the data from the neutrino-reconstruction and missing-mass methods, respectively. The solid line is the average of the form factor slopes from these two methods, and the dotted line has the slope $\hat{\rho}^2$ as obtained from the CLEO II measurement of $|V_{cb}|$ using $\bar{B} \rightarrow D^* \ell^- \bar{\nu}$.

likelihood fit to these variables. The analysis is performed in two modes, $\bar{B}^0 \rightarrow D^{*+} \ell^- \bar{\nu}$, which is fairly clean (779 ± 42 signal events over 161 ± 28 background events), and $B^- \rightarrow D^{*0} \ell^- \bar{\nu}$, which is somewhat more difficult (417 ± 33 signal events over a background of 270 ± 21 events).

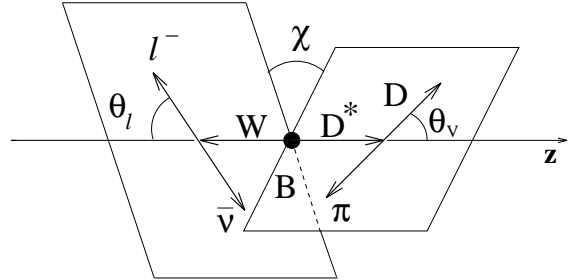


Figure 6: Decay angles used in the CLEO II measurement of the $\bar{B} \rightarrow D^* \ell^- \bar{\nu}$ form factors. The angle θ_ℓ is measured in the W rest frame, while θ_V is measured in the D^* rest frame. The azimuthal angle χ is measured between the W and D^* decay planes.

Figure 7 shows some of the fit projections for the combined $\bar{B} \rightarrow D^* \ell^- \bar{\nu}$ modes. The two upper histograms compare the distributions of $\cos \theta_V$ in the lower and upper half of the q^2 range. Although acceptance effects, which are taken into account in the fit, gradually reduce the efficiency as $\cos \theta_V$ increases, it is apparent that in the lower q^2 range there is a strong forward-backward-peaking component. At low q^2 , the lepton and antineutrino become collinear, with zero net spin along their common direction, forcing the D^* also to have

zero helicity. This effect produces a distribution $dN/d\cos\theta_V \propto \cos^2\theta_V$. In contrast, at very high q^2 , the D^* is nearly at rest and unpolarized, producing a $\cos\theta_V$ distribution that is uniform, apart from acceptance effects. The lower two histograms show distributions of the azimuthal angle χ for the lower and upper range of $\cos\theta_V$. The correlation between these histograms arises from a quantum interference term proportional to the difference between negative and positive helicity amplitudes, multiplied by the zero helicity amplitude. The upward slope of the first histogram (c) and the downward slope of the second histogram (d) are allowed by $(V-A)(V-A)$ or $(V+A)(V+A)$, but this correlation is forbidden by a mixed coupling $(V \mp A)(V \pm A)$.

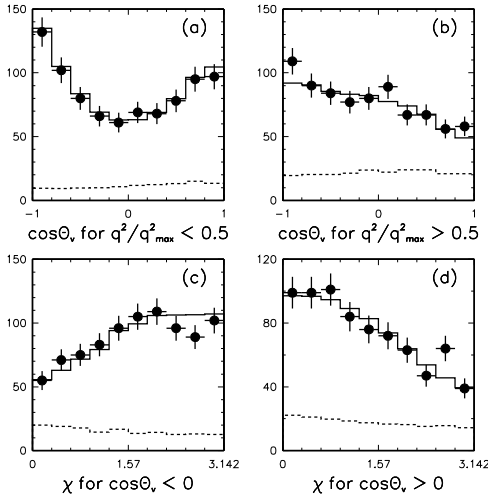


Figure 7: Distributions of $\cos\theta_V$ and χ in the CLEO II measurement of the $\bar{B} \rightarrow D^*\ell^-\bar{\nu}$ form factors. The histograms show (a) $\cos\theta_V$ for the lower half of the q^2 range, (b) $\cos\theta_V$ for the upper half of the q^2 range, (c) χ for the lower half of the $\cos\theta_V$ range, and (d) χ for the upper half of the $\cos\theta_V$ range. The points with error bars are the data; the solid histogram is the fit, including backgrounds; and the dashed line is the contribution from backgrounds. The interpretation of these histograms is discussed in the text.

In the framework of HQET, it is useful to construct quantities that have simple behavior in the heavy-quark symmetry limit. It is conventional to define⁷ the form-factor ratios

$$R_1(w) \equiv \left[1 - \frac{q^2}{(m_B + m_{D^*})^2} \right] \frac{V(q^2)}{A_1(q^2)}$$

$$R_2(w) \equiv \left[1 - \frac{q^2}{(m_B + m_{D^*})^2} \right] \frac{A_2(q^2)}{A_1(q^2)} \quad (5)$$

and the HQET version of the A_1 form factor, called h_{A_1} :

$$h_{A_1}(w) = \frac{2\sqrt{m_B m_{D^*}}}{(m_B + m_{D^*})} \frac{A_1(q^2)}{\left[1 - \frac{q^2}{(m_B + m_{D^*})^2} \right]}. \quad (6)$$

(The A_1 form factor is singled out because it contributes to all three helicity amplitudes and dominates the rate at high q^2 .) In the heavy-quark symmetry limit, $R_1(w) \rightarrow 1$ and $R_2(w) \rightarrow 1$, and $h_{A_1}(w) \rightarrow \xi(w)$, as can be seen from Eq. 4. The fit determines $R_1(w=1)$ and $R_2(w=1)$, as well as the dimensionless form factor slope $\rho_{A_1}^2$ of h_{A_1} . (Since the true form of $h_{A_1}(w)$ is not known, several different functions are tried in addition to a simple linear function with slope $\rho_{A_1}^2$. The details of these alternative fits are discussed in the references.^{30,31}) Table 2 compares the measured values for $R_1(1)$ and $R_2(1)$ obtained from the combined fit to $\bar{B}^0 \rightarrow D^{*+}\ell^-\bar{\nu}$ and $B^- \rightarrow D^{*0}\ell^-\bar{\nu}$ with theoretical predictions from Neubert,⁷ Close and Wambach,²³ and the ISGW2 model.³² Within errors, the measurements are in good agreement with the predictions, and they follow the expected pattern $R_1(1) > 1$ and $R_2(1) < 1$. (CLEO has published the fit results for $\bar{B}^0 \rightarrow D^{*+}\ell^-\bar{\nu}$ only; the values in Table 2 are obtained from a combined fit to both $\bar{B}^0 \rightarrow D^{*+}\ell^-\bar{\nu}$ and $B^- \rightarrow D^{*0}\ell^-\bar{\nu}$. These results are preliminary and are described in a paper submitted to this conference.)

The slope $\rho_{A_1}^2$ describes nonperturbative QCD physics and can only be calculated with methods such as lattice QCD or QCD sum rules, with typical values ranging from 0.5 to 1.0. It is closely related to another parameter, $\hat{\rho}^2$, which is extracted together with $|V_{cb}|$ in studies of $\bar{B} \rightarrow D^*\ell^-\bar{\nu}$. Such analyses, which use only the q^2 distribution, have been performed by ARGUS, CLEO, and the LEP experiments. Because the three form factors cannot be separated using the q^2 distribution only, $\hat{\rho}^2$ is the slope of a function $\mathcal{F}(w)$ that has complicated dependence on all three form factors. Neubert gives the relation³³ $\hat{\rho}^2 = \rho_{A_1}^2 - f(R_1, R_2)$, where the function $f(R_1, R_2) \approx 0.2$ for the values of R_1 and R_2 quoted above.

Figure 8 lists the form factor slopes for both $\bar{B} \rightarrow D\ell^-\bar{\nu}$ and $\bar{B} \rightarrow D^*\ell^-\bar{\nu}$. The first measurement is $\rho_{A_1}^2$ from the CLEO II four-dimensional

Table 2: CLEO II measurements of form factor ratios for $\bar{B} \rightarrow D^* \ell^- \bar{\nu}$ and comparison with theoretical predictions. The CLEO results are based on a combined fit to both $\bar{B}^0 \rightarrow D^{*+} \ell^- \bar{\nu}$ and $B^- \rightarrow D^{*0} \ell^- \bar{\nu}$ and are preliminary.

	$R_1(w=1)$	$R_2(w=1)$
CLEO II	$1.24 \pm 0.26 \pm 0.12$	$0.72 \pm 0.18 \pm 0.07$
Neubert	1.3 ± 0.1	0.8 ± 0.2
Close & Wambach	1.15	0.91
ISGW2	1.27	1.01

fit to the $\bar{B} \rightarrow D^* \ell^- \bar{\nu}$ kinematic distributions³¹; the second group of measurements is ρ^2 from the q^2 distribution of $\bar{B} \rightarrow D^* \ell^- \bar{\nu}$; and the third group is the slope of the form factor for $\bar{B} \rightarrow D \ell^- \bar{\nu}$. The average value of the second group, which consists of measurements from CLEO,³⁴ ARGUS,³⁵ ALEPH,²⁶ DELPHI,³⁶ and OPAL³⁷) is $\rho^2 = 0.75 \pm 0.11$, where the slightly inflated error takes into account the somewhat poor agreement among the measurements. As expected, this value is slightly lower than $\rho_{A_1}^2$, although the uncertainties are still too large to draw a strong conclusion. Furthermore, the slope for $\bar{B} \rightarrow D \ell^- \bar{\nu}$ is consistent with those measured for $\bar{B} \rightarrow D^* \ell^- \bar{\nu}$, although here again improvements in the uncertainties are very desirable.

CLEO II A1		$0.92 \pm 0.12 \pm 0.06$
CLEO II		$0.84 \pm 0.12 \pm 0.08$
ARGUS		$1.17 \pm 0.22 \pm 0.06$
ALEPH		$0.29 \pm 0.18 \pm 0.12$
DELPHI		$0.75 \pm 0.17 \pm 0.10$
OPAL		$0.44 \pm 0.24 \pm 0.00$
Average D*		0.75 ± 0.11
CLEO II		$0.64 \pm 0.18 \pm 0.10$
ALEPH		$0.00 \pm 0.49 \pm 0.38$
Average D		0.58 ± 0.20

Figure 8: Measurements of form factor slopes in $\bar{B} \rightarrow D^* \ell^- \bar{\nu}$ and $\bar{B} \rightarrow D \ell^- \bar{\nu}$. The top measurement is $\rho_{A_1}^2$ from the CLEO II four-dimensional fit to $\bar{B} \rightarrow D^* \ell^- \bar{\nu}$. Below it are measurements of ρ^2 from $\bar{B} \rightarrow D^* \ell^- \bar{\nu}$, which are expected to be slightly lower than $\rho_{A_1}^2$. The vertical dotted line corresponds to the average value of ρ^2 . The bottom group (CLEO II, ALEPH) is the slope measured in $\bar{B} \rightarrow D \ell^- \bar{\nu}$.

In summary, we can say that $R_1(1)$ and $R_2(1)$ are quite consistent with HQET predictions (they

Table 3: Measurements of $\bar{B} \rightarrow D^{**} \ell^- \bar{\nu}$ modes. The results marked with an asterisk* were submitted to this conference and are preliminary. The ALEPH $D_1 \ell^- \bar{\nu}$ measurement is an average over $D_1^+ \ell^- \bar{\nu}$ and $D_1^0 \ell^- \bar{\nu}$.

Expt	$B(B^- \rightarrow D_1^0 \ell^- \bar{\nu})$	$B(B^- \rightarrow D_2^{*0} \ell^- \bar{\nu})$
OPAL	$(2.02 \pm 0.51 \pm 0.47)\%$	$(0.88 \pm 0.35 \pm 0.18)\%$
ALEPH*	$(0.74 \pm 0.16)\%$	$< 1\% (95\% \text{ C.L.})$
CLEO II*	$(0.49 \pm 0.13 \pm 0.06)\%$	$< 1\% (95\% \text{ C.L.})$

are actually consistent with the heavy quark symmetry limit $R_1 = R_2 = 1$ itself), as are the relative sizes of form factor slopes for $\bar{B} \rightarrow D \ell^- \bar{\nu}$ and $\bar{B} \rightarrow D^* \ell^- \bar{\nu}$. With larger data samples, we can expect substantial improvements in these measurements.

Large values of $\rho_{A_1}^2$ (or $\hat{\rho}^2$) have an interesting consequence: the rates for $\bar{B} \rightarrow D \ell^- \bar{\nu}$ and $\bar{B} \rightarrow D^* \ell^- \bar{\nu}$ fall off faster with increasing recoil velocity, and the rates for $\bar{B} \rightarrow D^{**} \ell^- \bar{\nu}$ modes increase. For example, Dunietz gives the prediction³⁸

$$\frac{B(\bar{B} \rightarrow D^{**} \ell^- \bar{\nu})}{B(\bar{B} \rightarrow X_c \ell^- \bar{\nu})} \approx 2(\rho^2 - \frac{1}{4})(0.08 \pm 0.04). \quad (7)$$

New measurements of both $B(\bar{B} \rightarrow D_1 \ell^- \bar{\nu})$ and $B(\bar{B} \rightarrow D_2^* \ell^- \bar{\nu})$ were submitted to this conference by ALEPH³⁹ and CLEO.⁴⁰ Some of the results are listed in Table 3, along with earlier results from OPAL.⁴¹ In general, such measurements make assumptions regarding D_1 and D_2^* branching fractions and the absence of additional particles produced in the B decay, so some caution is advisable in interpreting the results.

3.3 Inclusive Semileptonic Branching Fraction

The inclusive semileptonic branching fraction is defined as

$$B_{\text{SL}} = \frac{\Gamma(\bar{B} \rightarrow X e^- \bar{\nu}_e)}{\sum_{\ell} \Gamma(\bar{B} \rightarrow X \ell^- \bar{\nu}) + \Gamma_{\text{Had}} + \Gamma_{\text{Rare}}}, \quad (8)$$

where Γ_{Had} and Γ_{Rare} are the partial widths to hadronic and rare final states. Most measurements of B_{SL} do not actually determine the b hadron species, because only the lepton is identified to keep the detection efficiency as high as possible. Thus, most measurements of B_{SL} at the $\Upsilon(4S)$ are an average over the \bar{B}^0 and B^- (with the notable exception of a new CLEO⁴² measurement submitted to this conference, which determines the value

of B_{SL} for \bar{B}^0 mesons). At the Z , the B_s and b baryons are included in the samples as well. Since b baryon lifetimes are typically shorter than those of B mesons, and it is reasonable to assume that the semileptonic rates are very similar, we expect the average b hadron semileptonic branching fraction measured at the Z to be slightly lower than that measured at the $\Upsilon(4S)$. As a reminder of this small difference, I will use the symbol B_{SL}^Z to refer to measurements performed at the Z .

Precise measurements of B_{SL} allow us to determine the fraction of exclusive semileptonic modes that have been identified. For the purpose of comparing the inclusive with the sum of exclusive semileptonic B branching fractions, I compute an average value of B_{SL} using the two measurements at the $\Upsilon(4S)$ that are based on the dilepton method, which has very little model dependence. Averaging the measurements from CLEO,⁴³ $B_{\text{SL}} = (10.49 \pm 0.17 \pm 0.43)\%$, and ARGUS,⁴⁴ $B_{\text{SL}} = (9.7 \pm 0.5 \pm 0.4)\%$, I obtain

$$B_{\text{SL}} = (10.23 \pm 0.39)\%. \quad (9)$$

For comparison, I also compute the average value of B_{SL}^Z , which is the semileptonic branching fraction for the b -hadron mixture produced in Z decays. I use measurements from ALEPH⁴⁵ $[(11.01 \pm 0.23 \pm 0.28 \pm 0.11)\%]$, DELPHI⁴⁶ $[(11.06 \pm 0.39 \pm 0.19 \pm 0.12)\%]$, L3⁴⁷ $[(10.85 \pm 0.12 \pm 0.43)\%]$, and OPAL⁴⁸ $[(10.5 \pm 0.6 \pm 0.4 \pm 0.3)\%]$, where the L3 value is a new result submitted to this conference, and the ALEPH result has the lesser model dependence of the two measurements presented in their paper. I assume a common systematic error of 0.25% (absolute). The resulting average, $B_{\text{SL}}^Z = (10.95 \pm 0.13 \pm 0.29)\%$, is somewhat lower than previous values of B_{SL}^Z , and it is more consistent with the value of B_{SL} measured at the $\Upsilon(4S)$.

To obtain averages of exclusive branching fractions from different experiments, it is important to use a common set of values for D and D^* branching fractions and, in the case of the LEP experiments, for $R_b = \Gamma(Z \rightarrow b\bar{b})/\Gamma(Z \rightarrow \text{hadrons})$ and $f_{b \rightarrow B}$, the fraction of b quarks that hadronize into a B^- or B^0 meson.²⁶ Table 4 lists the values that I have assumed for these quantities. The $D^0 \rightarrow K^-\pi^+$ branching fraction is the average that I calculate below, while the $D^+ \rightarrow K^-\pi^+\pi^+$ branching fraction has been scaled to take into account its experimental dependence on the $D^0 \rightarrow$

Table 4: Assumed values for quantities used to calculate averages of semileptonic branching fractions.

$B(D^0 \rightarrow K^-\pi^+)$	$(3.88 \pm 0.10)\%$
$B(D^+ \rightarrow K^-\pi^+\pi^+)$	$(8.8 \pm 0.6)\%$
$B(D^{*+} \rightarrow D^0\pi^+)$	$(68.1 \pm 1.6)\%$
$f_{b \rightarrow B}$ (LEP)	$(37.8 \pm 2.2)\%$
R_b (LEP)	$(22.09 \pm 0.21)\%$

$K^-\pi^+$ value. The $D^{*+} \rightarrow D^0\pi^+$ branching fraction is taken from the 1994 Particle Data Book,²⁹ but I have corrected the error, which was listed incorrectly in that reference.

Table 5 summarizes the status of semileptonic branching fractions. For $\bar{B} \rightarrow D^*\ell^-\bar{\nu}$, I compute a world average based on measurements at the $\Upsilon(4S)$ (CLEO³⁴ and ARGUS^{35,49}) and at the Z (ALEPH²⁶, DELPHI³⁶, OPAL³⁷). For the semileptonic branching fraction to $b \rightarrow c\ell^-\bar{\nu}$ modes other than $\bar{B} \rightarrow D\ell^-\bar{\nu}$ and $\bar{B} \rightarrow D^*\ell^-\bar{\nu}$, I use a measurement from ALEPH based on a topological vertex study.³⁹ This measurement determines $B(b \rightarrow \bar{B}) \times B(\bar{B} \rightarrow D^{*+}\pi^-\ell^-\bar{\nu}X) = (4.73 \pm 0.77 \pm 0.55) \times 10^{-3}$, as well as analogous branching fractions for final states with $D^{*0}\pi^+$, $D^+\pi^-$, and $D^0\pi^+$. Combining all of these results, ALEPH obtains $B(\bar{B} \rightarrow D\pi X\ell^-\bar{\nu} + \bar{B} \rightarrow D^*\pi X\ell^-\bar{\nu})$, where both resonant and nonresonant hadronic final states are included and $\bar{B} \rightarrow D\ell^-\bar{\nu}$ and $\bar{B} \rightarrow D^*\ell^-\bar{\nu}$ are excluded. (I have rescaled their result using the new $D^0 \rightarrow K^-\pi^+$ branching fraction.) For $b \rightarrow u\ell^-\bar{\nu}$, I have made a rough estimate (with 50% uncertainty) based on the value of $|V_{ub}|$ and the free quark model prediction.⁵⁰ The sum of all these branching fractions is $(9.38 \pm 0.65)\%$, about 1.2σ lower than the inclusive semileptonic branching fraction. This comparison shows that a fairly large fraction of the semileptonic rate is accounted for. It is clear, however, the much work remains in improving the precision of the branching fraction measurements and, in particular, obtaining a detailed understanding of the $\bar{B} \rightarrow D^{*+}\ell^-\bar{\nu}$ modes and modes with non-resonant final states.

The semileptonic branching fraction is also of great interest because it tests our understanding of the hadronic rate. Although there are significant theoretical uncertainties due to quark masses and the renormalization scale, important progress has

Table 5: Contributions to the B meson inclusive semileptonic branching fraction.

Mode	$B_i(\%)$
$B^0 \rightarrow D^+ \ell^- \bar{\nu}$	2.03 ± 0.28
$\bar{B}^0 \rightarrow D^{*+} \ell^- \bar{\nu}$	4.86 ± 0.29
$[(\bar{B} \rightarrow D\pi X \ell^- \bar{\nu})$ $+(\bar{B} \rightarrow D^*\pi X \ell^- \bar{\nu})]$	2.34 ± 0.45
$\bar{B} \rightarrow X_u \ell^- \bar{\nu}$	0.15 ± 0.075
ΣB_i	9.38 ± 0.65
$B_{\text{SL}}(4S)$	10.23 ± 0.39
$B_{\text{SL}}(4S) - \Sigma B_i$	0.85 ± 0.76

been made. The semileptonic branching fraction could also be sensitive to an anomalously large rate for $b \rightarrow sg$, which has been suggested by some theorists⁵¹.

Historically, most predictions of B_{SL} have been larger than the values measured at the $\Upsilon(4S)$. Recent calculations performed within the framework of $1/m_Q$ expansions have focused attention on this issue. For example, Bigi *et al.*⁵² have concluded that it is very difficult to obtain a prediction for B_{SL} below 12.5%. Various aspects of the problem have now been scrutinized in more detail, and Bagan *et al.*^{53,54} and Voloshin⁵⁵ have shown that higher order perturbative QCD corrections significantly increase the rate for $b \rightarrow c\bar{c}s$, thereby decreasing B_{SL} . To test this idea, one can measure n_c , the average number of charm (or anti-charm) quarks per B decay. Thus, what was originally posed as the problem of the semileptonic branching fraction is now regarded as the joint problem of B_{SL} and n_c . Bagan *et al.*⁵⁴ obtain $B_{\text{SL}} = (12.0 \pm 0.7 \pm 0.5 \pm 0.2^{+0.9}_{-1.2})\%$, where the errors are due to uncertainties in m_b , α_s , the b -quark kinetic energy parameter λ_1 , and the renormalization scale. In an alternative scheme with $\overline{\text{MS}}$ quark masses, they obtain $\bar{B}_{\text{SL}} = (11.3 \pm 0.6 \pm 0.7 \pm 0.2^{+0.9}_{-1.7})\%$. They also predict $n_c = 1.24 \pm 0.05 \pm 0.01$, where the first error is due to the uncertainty in m_b . The alternative $\overline{\text{MS}}$ calculation gives $n_c = 1.30 \pm 0.03 \pm 0.03 \pm 0.01$.

Experimentally, the quantity n_c is difficult to determine because one must identify and measure all final states in B decay that contain one or more charm quarks. Inclusive production of D^0 , D^+ , D_s , and J/ψ is relatively easy to measure, but the contributions from other charmonium states

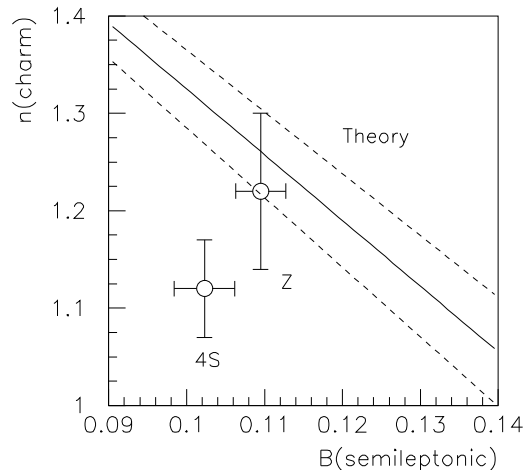


Figure 9: Comparison of n_c vs. B_{SL} for measurements at the $\Upsilon(4S)$ and the Z with theoretical prediction.

and from charm baryons are more difficult to determine. To compare results from different experiments, it is important to use a common set of charm branching fractions. I have updated the relevant CLEO II and ARGUS B branching fractions, which are listed in Browder *et al.*⁶, to reflect the charm branching fractions used in this article. In summing the B branching fractions, I take into account the correlated systematic error arising from common charm branching fractions. I have applied the same procedure to new data from the ALEPH experiment.⁵⁶ The values are

$$n_c(4S) = 1.12 \pm 0.05 \quad n_c^Z = 1.22 \pm 0.08, \quad (10)$$

where n_c^Z refers to the ALEPH measurement and is a reminder that the b hadron content at the Z is more complicated than at the $\Upsilon(4S)$. (This is seen, for example, in a significantly higher D_s^+ contribution at the Z than at the $\Upsilon(4S)$.) The error on the ALEPH measurement is larger than they report because I use the newer $D_s^+ \rightarrow \phi\pi^+$ branching fraction discussed later in this paper. OPAL⁵⁷ has reported the value $n_c^Z = 1.100 \pm 0.045 \pm 0.060$, which I have not updated to the new D^0 and D_s^+ branching fractions.

Figure 9 compares the points $(B_{\text{SL}}, n_c(4S))$ and (B_{SL}^Z, n_c^Z) with the theoretical summary given in Buchalla *et al.*⁵⁸. My view is that, given the size of the present experimental and theoretical uncertainties, we cannot state that there is or is not a problem in explaining the measured value of B_{SL} .

There have already been substantial refinements in both experimental and theoretical analyses of this question, and it is important to continue these studies until the issue is resolved.

4 Hadronic Decays of Charm and Bottom Mesons

4.1 Normalization modes for the D^0 and D_s^+

The branching fractions for the decays $D^0 \rightarrow K^- \pi^+$ and $D_s^+ \rightarrow \phi \pi^+$ are crucial for many measurements in charm and bottom physics, since they ultimately determine the absolute branching fraction scales. A new high-precision measurement of $D^0 \rightarrow K^- \pi^+$ from ALEPH was submitted to this conference.⁵⁹ The key to this analysis, like those of earlier measurements from the HRS,⁶⁰ ARGUS,⁶¹ and CLEO,⁶² is to tag $D^{*+} \rightarrow D^0 \pi^+$ without using the D^0 decay products. The tag is based on the fact that the energy release in the D^{*+} decay is extremely low, about 6 MeV. In the D^{*+} rest frame, the resulting “soft pion” has momentum $p_\pi^* \approx 40$ MeV/c, which limits its transverse momentum relative to the D^{*+} direction in the lab frame. This low p_T pion provides a distinctive signature for the D^{*+} decay. Since the p_T measurement must be performed without reconstructing the full D^{*+} decay chain, the D^{*+} direction is approximated by the jet axis. To determine $B(D^0 \rightarrow K^- \pi^+)$, one then measures the fraction of such tags in which the decay $D^0 \rightarrow K^- \pi^+$ is found. A key part of this measurement is to accurately determine the background shape in p_T that arises from soft pions due to other sources. Figure 10 shows the ALEPH p_T^2 distributions, which have peaks at the low end due to $D^{*+} \rightarrow D^0 \pi^+$.

Figure 11 summarizes the status of $D^0 \rightarrow K^- \pi^+$ measurements. The new preliminary result from ALEPH is somewhat more precise than the CLEO II measurement, and the two values are quite consistent. The average of all the measurements is $B(D^0 \rightarrow K^- \pi^+) = (3.88 \pm 0.10)\%$, which I use in several places in this paper. Recently, Dunietz³⁸ has argued that a lower value of this branching fraction is indicated by a number of problems in B physics. This conclusion is not supported by the new ALEPH result, but it is extremely important that the $D^0 \rightarrow K^- \pi^+$ branching fraction be checked by other experiments.

Measurements of $B(D_s^+ \rightarrow \phi \pi^+)$ are much less

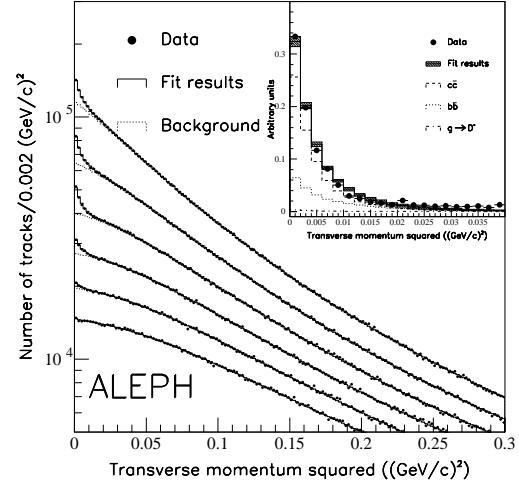


Figure 10: ALEPH measurement of $B(D^0 \rightarrow K^- \pi^+)$. The data points show the distribution of transverse momentum squared of hadrons, relative to the axis of the nearest jet, in six pion momentum bins from 1 GeV/c at the top to 4 GeV/c at the bottom. The peaks at the low end of the distributions are due to the soft pion from the decay $D^{*+} \rightarrow D^0 \pi^+$. The figure in the upper-right corner shows the background-subtracted p_T^2 distribution after the data from all six pion momentum bins are combined.

precise. The 1994 version of the Particle Data Book²⁹ lists $B(D_s^+ \rightarrow \phi \pi^+) = (3.5 \pm 0.4)\%$. However, this value is based mainly on measurements of $\Gamma(D_s^+ \rightarrow \phi \pi^+)/\Gamma(D_s^+ \rightarrow \phi \ell^+ \nu)$. The scale is then set by assuming that $\Gamma(D_s^+ \rightarrow \phi \ell^+ \nu)$ and $\Gamma(D \rightarrow K^* \ell^+ \nu)$ are equal, up to a small theoretical correction. The new CLEO II measurement⁶³ of the absolute branching fraction avoids any theoretical assumptions. In this measurement, the decay $\bar{B}^0 \rightarrow D^{*+} D_s^{*-}$ is reconstructed in two ways: (1) the D_s^{*-} is fully reconstructed and the D^{*+} is partially reconstructed using the soft pion from

MARK I		$(4.3 \pm 1.0)\%$
MARK II		$(4.1 \pm 0.6)\%$
MARK III		$(4.2 \pm 0.4 \pm 0.4)\%$
HRS		$(4.5 \pm 0.8 \pm 0.5)\%$
ARGUS		$(4.5 \pm 0.6 \pm 0.4)\%$
CLEO II		$(3.91 \pm 0.08 \pm 0.17)\%$
ARGUS		$(3.41 \pm 0.12 \pm 0.28)\%$
ALEPH		$(3.90 \pm 0.09 \pm 0.12)\%$
Average		$(3.88 \pm 0.10)\%$

Figure 11: Summary of measurements of $B(D^0 \rightarrow K^- \pi^+)$.

$D^{*+} \rightarrow D^0 \pi^+$, and (2) the D^{*+} is fully reconstructed and the D_s^{*-} is partially reconstructed using the soft photon from $D_s^{*-} \rightarrow D_s^- \gamma$. CLEO obtains $B(D_s^+ \rightarrow \phi \pi^+)/B(D^0 \rightarrow K^- \pi^+) = 0.92 \pm 0.20 \pm 0.11$, which is the basis for the 1996 Particle Data Book¹⁵ value $B(D_s^+ \rightarrow \phi \pi^+) = (3.6 \pm 0.9)\%$. The quoted uncertainty is significantly larger than before, but no theoretical assumptions are made.

4.2 Hadronic B Decays and Factorization

Hadronic decays are much more complicated than leptonic or semileptonic modes, because all of the fermions involved are quarks and can interact strongly. Although it is not possible to make precise predictions for hadronic decays, the factorization hypothesis provides a framework for understanding many of the observed features of two-body modes. In the factorization approach, one writes the decay amplitude as the product of two currents, in analogy to semileptonic decay. Factorization was discussed extensively at this conference by several experimentalists,^{64,65,66} and these talks led to considerable discussion regarding the applicability and reliability of factorization in various decay processes. Here, I will only give an introduction to some of the experimental results related to this complex topic.

Figure 12 shows the hadronic decay of a B meson through (a) an external spectator diagram and (b) an internal (color suppressed) spectator diagram. In the factorization approach, the effects of strong interactions are divided into two categories: (1) short-distance, hard-gluon effects parametrized by the coefficient a_1 for the external diagram and a_2 for the internal diagram and (2) long-distance, soft-gluon effects, which are parametrized by decay constants and form factors. In Fig. 12(a) the $\bar{u}d$ system from the W decay is produced at a point, so that the appropriate meson decay constant, which measures the overlap of the quark anti-quark pair, parametrizes the amplitude to produce the meson. To be definite, we take this meson to be a pion. The daughter charm quark recoiling at the lower W vertex, however, must bind together with the spectator quark. The physics of this process is very similar to the hadronic transition in semileptonic decay discussed earlier, and it is described by the appropriate form factor evaluated at $q^2 = m_\pi^2$. Thus, for the external spectator diagram example, the non-perturbative QCD

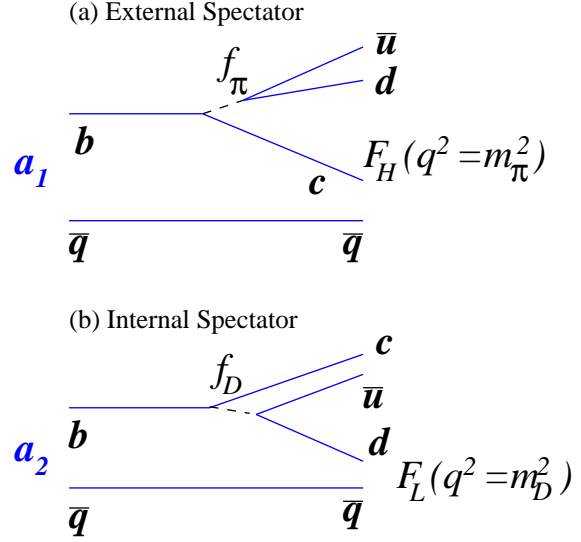


Figure 12: Spectator diagrams for B decays with (a) an external W and (b) an internal W . The QCD hard-gluon corrections are parametrized by the coefficients a_1 and a_2 , while nonperturbative effects are described, in our $B \rightarrow D\pi$ example, by the decay constant f_π or f_D and the form factor $F_H(q^2 = m_\pi^2)$ or $F_L(q^2 = m_D^2)$.

physics is described by the pion decay constant f_π and a “heavy-to-heavy” ($B \rightarrow X_c$) form factor $F_H(q^2 = m_\pi^2)$.

For a_1 -type decays with large daughter-hadron recoil velocity (i.e., decays at low q^2), one might expect factorization to be a good approximation from the following argument, due to Bjorken.⁶⁷ The $q\bar{q}$ pair produced in the W decay is formed at a point as a color singlet, and, for low q^2 processes, the pair moves out of the decaying hadron at high velocity in a collinear fashion. Thus, the pair looks like a very small color dipole that gradually grows to the size of a meson. The pair will not form a meson, however, until it moves a distance $\approx \gamma c \tau_h$, where τ_h is a typical hadronization time in the rest frame, $\tau_h \sim 1 \text{ fm}/c$. This distance can be as large as 20 fm, much larger than the decaying meson, so that the pair can escape from the cloud of quarks and gluons without significantly interacting with it.

Consider now the internal spectator diagram, shown in Fig. 12. Because the W has such a short range compared with the size of a hadron, the c and the \bar{u} are still effectively produced at the same point, and the relevant decay constant is f_D instead of f_π . It is the daughter d quark that now

must bind with the spectator, so there is now a “heavy-to-light” ($B \rightarrow X_u$) form factor, which I denote by $F_L(q^2 = m_D^2)$.

For a \bar{B}^0 decay, the external and internal diagrams lead to different final states (charged+charged and neutral+neutral), whereas in B^- decay two \bar{u} quarks are present in the final state, which means that the same charged+neutral final state can be reached in two ways. Thus, we have the pattern

$$\begin{aligned} \bar{B}^0(b\bar{d}) &\rightarrow \text{chg} + \text{chg} : \Gamma \propto |a_1 f_\pi F_H|^2 \\ \bar{B}^0(b\bar{d}) &\rightarrow \text{neut} + \text{neut} : \Gamma \propto |a_2 f_D F_L|^2 \\ B^-(b\bar{u}) &\rightarrow \text{chg} + \text{neut} : \\ &\Gamma \propto |a_1 f_\pi F_H + a_2 f_D F_L|^2 \end{aligned} \quad (11)$$

Using measured branching fractions for hadronic B decays, one can extract the coefficients a_1 and a_2 arising from hard gluon effects. This procedure requires knowledge of both decay constants and form factors. As discussed earlier, our knowledge of these quantities is far from perfect, especially in the case of the form factors for heavy-to-light transitions. Compared with the state of our understanding of hadronic decays, however, form factor predictions might be regarded as reasonably trustworthy, but it is important to remember that there is more uncertainty in calculations made within the factorization framework than is often acknowledged.

One approach to testing factorization is to compare the decay rate for a hadronic mode with the rate at the same value of q^2 for a semileptonic decay. For $B \rightarrow D^{(*)}P$ decays, where P is a pseudoscalar meson, one can define⁶⁸ the ratio

$$\begin{aligned} R_P^{(*)} &= \frac{\Gamma(\bar{B} \rightarrow D^{(*)}P)}{d\Gamma(\bar{B} \rightarrow D^{(*)}\ell^-\bar{\nu})/dq^2|_{q^2=m_P^2}} \\ &= 6\pi^2 f_P^2 a_1^2 |V_{ij}|^2 X_P^{(*)}(q^2 = m_P^2), \end{aligned} \quad (12)$$

where $X_P^{(*)}$ is the ratio of form factors for the hadronic to the semileptonic decay. (This ratio is defined in Neubert *et al.*⁶⁸ In most cases, $X_P^{(*)}$ is approximately equal to one. However, the semileptonic decay form factor that becomes important only for large lepton mass is the one that enters into the hadronic decay, so there can be some subtleties here.)

The upper line of Eq. 12 can be evaluated from experiment, while the lower line can be calculated from theory, the comparison giving a test

Table 6: Values of a_1 extracted from a comparison of hadronic and semileptonic B decays. The consistency of these values is an indication of whether factorization provides a good description of the hadronic decays.

Mode	a_1
$\bar{B}^0 \rightarrow D^+\pi^-$	0.92 ± 0.10
$\bar{B}^0 \rightarrow D^+\rho^-$	0.97 ± 0.13
$\bar{B}^0 \rightarrow D^{*+}\pi^-$	0.96 ± 0.10
$\bar{B}^0 \rightarrow D^{*+}\rho^-$	0.92 ± 0.12
$\bar{B}^0 \rightarrow D^{*+}a_1^-$	1.1 ± 0.13
$\bar{B}^0 \rightarrow D^{(*)+}D_s^{(*)-}$	1.24 ± 0.40

of whether factorization is valid. The constant a_1 can be calculated from QCD: $a_1 = c_1 + c_2/3 \approx 1.0$, where c_1 and c_2 are calculated using the renormalization group equation. However, I prefer to use Eq. 12 to extract a_1 for different decay modes and then to check whether the resulting values are consistent.

Table 6 shows the values of a_1 for a set of \bar{B}^0 decay modes that can be compared with $\bar{B}^0 \rightarrow D^+\ell^-\bar{\nu}$ and $\bar{B}^0 \rightarrow D^{*+}\ell^-\bar{\nu}$. The agreement among these values is reasonably good, indicating that at the low values of q^2 (fast recoil) at which these hadronic decays occur, factorization provides a good description of the process. The data for the comparison with $\bar{B} \rightarrow D\ell^-\bar{\nu}$ are taken from the CLEO²⁵, while the $\bar{B} \rightarrow D^*\ell^-\bar{\nu}$ comparison is made using combined CLEO and ARGUS data compiled in Browder *et al.*⁶. The data for the $\bar{B}^0 \rightarrow D^{(*)+}D_s^{(*)-}$ are from CLEO⁶⁹ and assume $f_{D_s} = f_{D_s^*}$.

Another interesting test of factorization is to compare the polarization of the D^* in the hadronic decay $\bar{B}^0 \rightarrow D^{*+}\rho^-$ with that in the semileptonic decay $\bar{B}^0 \rightarrow D^{*+}\ell^-\bar{\nu}$, when measured at the same value of q^2 . In a semileptonic decay at low q^2 , the lepton and antineutrino are nearly collinear, so their net spin along their direction of motion is zero. Since the B has spin zero, the recoiling meson must also have helicity zero. In the factorization picture, the quark-antiquark pair from the W would behave like the lepton-antineutrino system, so that the ρ^- (or D^{*+}) is expected to be almost completely longitudinally polarized. The new CLEO II measurement³¹ of the $\bar{B} \rightarrow D^*\ell^-\bar{\nu}$ form factors gives $(\Gamma_L/\Gamma)_{q^2=m_\rho^2} = (91 \pm 1.3 \pm 0.6)\%$. For $\bar{B}^0 \rightarrow D^{*+}\rho^-$, CLEO ob-

tains⁷⁰ $\Gamma_L/\Gamma = (93 \pm 5 \pm 5)\%$, a very similar value.

We can also compare the decay rates for $\bar{B}^0 \rightarrow D^{*+}\rho^-$ and $\bar{B}^0 \rightarrow D^+\rho^-$. One might expect the rate for the $D^{*+}\rho^-$ to be larger, because there are more spin states accessible. However, factorization predicts that the rates should be about the same, since the D^{*+} polarization is almost completely longitudinal (helicity zero). The PDG96¹⁵ values are $B(\bar{B}^0 \rightarrow D^{*+}\rho^-) = (0.73 \pm 0.15)\%$ and $B(\bar{B}^0 \rightarrow D^+\rho^-) = (0.78 \pm 0.14)\%$, which are indeed very similar.

Although factorization is on a less secure footing for color-suppressed processes, there is great interest in the ratio a_2/a_1 , whose sign manifests itself in the interference term in B^- decays. The magnitude of a_2 can also be determined from color-suppressed \bar{B}^0 decays, such as $\bar{B}^0 \rightarrow J/\psi K^{0(*)}$. Skwarnicki⁶⁶ presented new CLEO II measurements of $B(\bar{B}^0 \rightarrow D^{*+}\pi^-)$ and $B(B^- \rightarrow D^{*0}\pi^-)$ that are based on a novel partial reconstruction technique, resulting in smaller statistical errors. From the ratio of these branching fractions, he extracts $a_2/a_1 = +(0.27 \pm 0.03)$, which differs substantially from the value in charm decays, where a_2/a_1 is negative. As discussed earlier, the error does not include all theoretical uncertainties. The long D^+ lifetime (relative to that of the D^0 or D_s^+) is attributed to the negative value of a_2/a_1 ; the positive value in B decays would indicate a shorter B^+ than B^0 lifetime, although the importance of two-body decays (from which this ratio is obtained) may be less in B decays.

4.3 Rare Hadronic Decays

Experiments are now achieving sensitivities to B branching fractions in the range 10^{-4} to 10^{-5} , opening up new types of processes for study. Here I will focus on rare decays to hadronic final states; electromagnetic penguins are covered in the talk by A. Buras.

Many rare hadronic decays, such as $B \rightarrow \pi\pi$ and $B \rightarrow K\pi$, can proceed either through a $b \rightarrow u$ spectator diagram or through a gluonic penguin. In the latter process, a $b \rightarrow d$ or $b \rightarrow s$ transition occurs through a virtual loop containing a W and either a t or c quark, with the radiation of a gluon. The theoretical expectation is that the decays $\bar{B}^0 \rightarrow \pi^+\pi^-$ and $\bar{B}^0 \rightarrow \pi^+\rho^-$ are dominated by the $b \rightarrow u$ spectator process, while

$\bar{B}^0 \rightarrow K^-\pi^+$ and $\bar{B}^0 \rightarrow K^{*-}\pi^+$ are dominated by $b \rightarrow sg$. The gluonic penguins are of interest not only as one-loop processes, but also because they can affect studies of CP violation. For example, the final state in $\bar{B}^0(B^0) \rightarrow \pi^+\pi^-$ is an eigenstate of the CP operator, and this decay is well suited to the measurement of $\sin 2\alpha$, where α is one of the angles of the CKM unitarity triangle. However, a significant contribution to this mode from $b \rightarrow dg$ would complicate the interpretation of the CP asymmetry and is sometimes called “penguin pollution.” Measurements of the relative size of branching fractions to non-strange and strange final states would provide information on the level of this contamination and are therefore of great interest for CP violation studies.

A simple argument gives some idea of the possible level of penguin contamination. Assuming that the t -quark dominates the loop, the penguin contribution to $\bar{B}^0 \rightarrow \pi^+\pi^-$ is suppressed relative to that for $\bar{B}^0 \rightarrow K^-\pi^+$ by $|V_{td}/V_{ts}|^2 = \mathcal{O}(\lambda^2)$, where $\lambda \simeq 0.22$ is the sine of the Cabibbo angle. Furthermore, the spectator contribution to $\bar{B}^0 \rightarrow K^-\pi^+$ is suppressed relative to that for $\bar{B}^0 \rightarrow \pi^+\pi^-$ by a factor $|V_{us}/V_{ud}|^2 \simeq \lambda^2$. Now, suppose that $B(\bar{B}^0 \rightarrow \pi^+\pi^-) \approx B(\bar{B}^0 \rightarrow K^-\pi^+)$, as is crudely indicated by experiment. Then our CKM argument implies that $\bar{B}^0 \rightarrow K^-\pi^+$ must be mainly penguin, or else the $\pi^+\pi^-/K^-\pi^+$ ratio would be larger. Furthermore, even if all of the $\bar{B}^0 \rightarrow K^-\pi^+$ rate were penguin, the (assumed) near equality of the branching fractions implies that the penguin contribution to $\bar{B}^0 \rightarrow \pi^+\pi^-$ must be fairly small, since this contribution is suppressed by λ^2 relative to the penguin contribution to $\bar{B}^0 \rightarrow K^-\pi^+$.

CLEO has updated⁷¹ its original measurement of the sum of rates to $\pi^-\pi^+$ and $K^-\pi^+$:

$$\begin{aligned} B(\bar{B}^0 \rightarrow \pi^-\pi^+ + K^-\pi^+) \\ = (1.8_{-0.5}^{+0.6+0.2} \pm 0.2) \times 10^{-5}. \end{aligned} \quad (13)$$

There are about 17 events in the signal, with a significance of 4σ to 5σ . Due to the high momentum of the decay products, the π/K separation is difficult, and the two modes are not clearly distinguished. CLEO reports $R = N_{\pi\pi}/(N_{\pi\pi} + N_{K\pi}) = 0.54_{-0.20}^{+0.19} \pm 0.05$. The systematic error on R is relatively small, so it will be possible to substantially improve the separation between the modes with additional data.

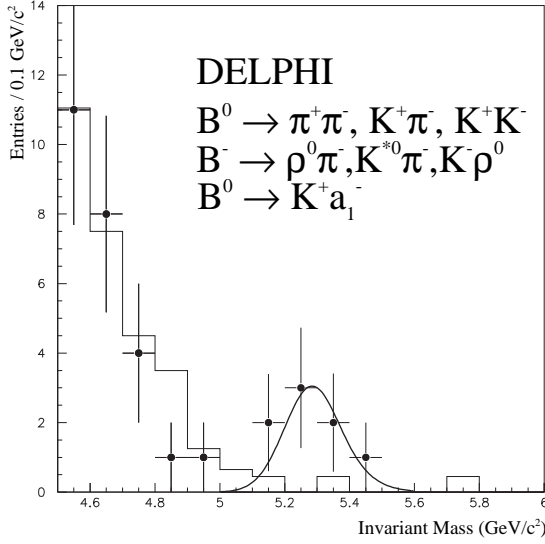


Figure 13: DELPHI data on two-body hadronic B decays to charmless final states. The points with error bars show the distribution of invariant masses for the data; the histogram shows the expectation if there were no charmless B decays, as predicted from Monte Carlo. The curve represents the signal shape normalized to the data.

DELPHI and ALEPH both presented new results on rare b hadron decays. The DELPHI analysis⁷² benefits from good particle identification from their ring-imaging Cerenkov detector (RICH). They observe eight events, of which five are in the two-prong subsample ($\pi^+\pi^- + K^+\pi^-$) and three are in the three-prong subsample ($\rho\pi + K^*\pi$). Within the two-prong subsample, three events are from $K^+\pi^-$. DELPHI also determines that the B_s contribution to this sample is relatively small, about 1.3 events. They obtain $B(B_{d,s}^0 \rightarrow \pi^+\pi^-, K^+\pi^-) = (2.8^{+1.5}_{-1.0} \pm 0.2) \times 10^{-5}$, consistent with CLEO, and

$$\frac{(B_{u,d} \rightarrow K\pi, K^*\pi)}{(B_{u,d} \rightarrow \pi\pi, \rho\pi) + (B_{u,d} \rightarrow K\pi, K^*\pi)} = 0.58 \pm 0.18. \quad (14)$$

Figure 13 shows the invariant mass spectrum from DELPHI for candidate two- and three-prong events. ALEPH⁷³ also presented results from a search for rare hadronic decays; they find four signal events and obtain $B(B \rightarrow h^+h^-) = (1.7^{+1.0}_{-0.7} \pm 0.2) \times 10^{-5}$, where the initial state can include B^0 , B_s , and Λ_b .

CLEO presented evidence⁷⁴ for a new rare decay, $B^+ \rightarrow \omega h^+$, where $h^+ = \pi^+$ or K^+ . Figure 14

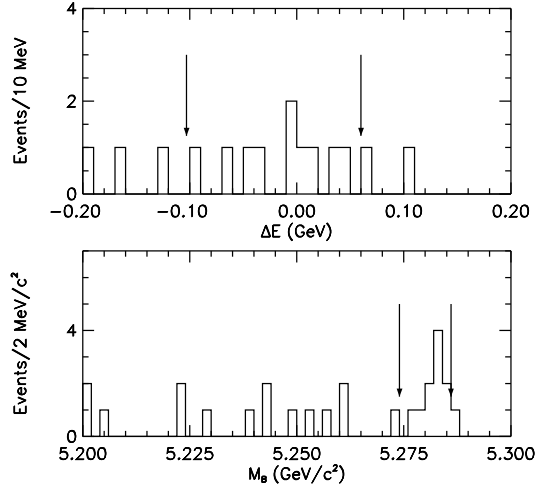


Figure 14: CLEO II measurement of $B^- \rightarrow \omega h^-$. The upper histogram shows the distribution of ΔE , the difference between the total energy of the candidate particles and the beam energy. The lower histogram shows the distribution of beam-energy constrained masses. The arrows indicate the signal regions in these two variables.

shows the distributions of $\Delta E = E_\omega + E_h - E_{\text{beam}}$ and $M(\omega h^+) = \sqrt{E_{\text{beam}}^2 - (\mathbf{p}_{\omega h})^2}$; these variables have resolutions $\sigma_{\Delta E} \approx 30$ MeV and $\sigma_{M_B} \approx 3$ MeV. A peak is evident in the $M(\omega h^+)$ distribution at the B mass, as is a broad cluster of events centered around $\Delta E = 0$. The arrows in the plots indicate the signal region, which contains a total of 10 events with an estimated background (due to continuum) of 2 events. CLEO obtains the preliminary result $B(B^+ \rightarrow \omega h^+) = (2.8 \pm 1.0 \pm 0.6) \times 10^{-5}$.

Many other results were presented on rare B decays, including an update on $b \rightarrow s\gamma$ branching fractions from CLEO,⁷⁵ limits on $b \rightarrow s\gamma$ and $b \rightarrow s\nu\bar{\nu}$ from DELPHI,⁷² limits on inclusive modes sensitive to $b \rightarrow sg$ from CLEO,⁷⁶ and limits on other hadronic rare decays from CLEO.^{77,78} The study of rare B decays is at an early stage, with only handfuls of events observed so far in exclusive modes. As very large data samples are accumulated at B factories in the future, we can expect many new results on these decays.

5 Lifetimes of b Hadrons

Measurements of \bar{B}^0 and B^- lifetimes are reaching an impressive precision, with systematic errors as small as ± 0.02 ps (CDF), and total errors for individual measurements as small as ± 0.06 ps (DELPHI). There are also substantial improvements in the lifetime measurements for both the B_s and Λ_b .

Predictions for the ratios of b -hadron lifetimes have been made by many theorists. I will make only a few comments, leaving the detailed theoretical discussion to the talk by Martinelli. Using the heavy-quark expansion, Neubert obtains¹⁰

$$\begin{aligned}\frac{\tau(B^-)}{\tau(B^0)} &= 1 + \mathcal{O}(1/m_b^3), \\ \frac{\tau(B_s)}{\tau(B^0)} &= (1.00 \pm 0.01) + \mathcal{O}(1/m_b^3), \\ \frac{\tau(\Lambda_b)}{\tau(B^0)} &\simeq 0.98 + \mathcal{O}(1/m_b^3),\end{aligned}\quad (15)$$

where the estimate for $\tau(\Lambda_b)/\tau(B^0)$ includes corrections that arise at order $1/m_b^2$. Although these ratios might appear very close to unity, Neubert argues that the $1/m_b^3$ corrections to $\tau(B^-)/\tau(B^0)$ might be large (due to phase-space enhancement of effects involving the spectator quark), and he concludes that theoretical uncertainties allow a lifetime ratio in the range $0.8 < \tau(B^-)/\tau(B^0) < 1.2$. This subject is controversial, and other theorists have placed tighter constraints on this ratio. For example, Bigi⁹ concludes that the B^- lifetime is definitely longer than the B^0 lifetime:

$$\frac{\tau(B^-)}{\tau(B^0)} \simeq 1 + 0.05 \cdot \frac{f_B^2}{(200 \text{ MeV})^2}. \quad (16)$$

There is more consensus on $\tau(B_s)/\tau(B^0)$, which is expected to be unity up to corrections of order 1%. Theoretical estimates for $\tau_{\Lambda_b}/\tau_{B^0}$ are typically in the range 0.9 to 1.0.

Lifetime measurements can be grouped into three broad categories, corresponding to the use of semileptonic decays, fully reconstructed hadronic decays, and inclusive methods such as topological vertexing. The main advantages of using semileptonic decays, such as $\bar{B} \rightarrow D^{(*)}\ell^-(X)\bar{\nu}$, are the large branching fractions, the presence of the lepton, and good vertex determination. There are, however, significant disadvantages. Because there is always at least one missing particle, the neutrino, it is generally not possible to reconstruct a

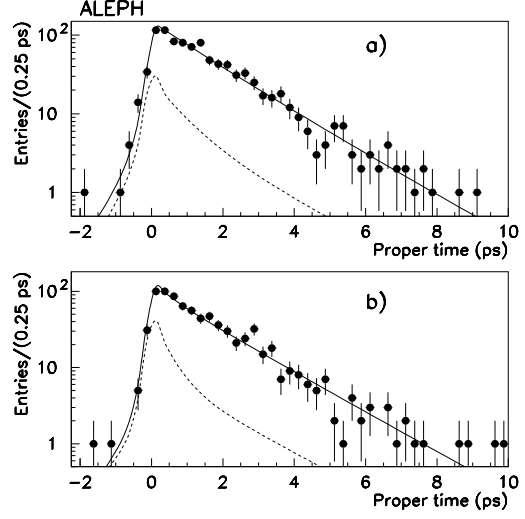


Figure 15: Proper time distribution for the ALEPH measurement of $\tau(B^-)$ and $\tau(B^0)$ using semileptonic B decay. The points with errors show the data for (a) $D^{*+}\ell^-$ events and (b) $D^0\ell^-$ events, which correspond mainly the B^0 and B^- decays. The dashed curves represent the background contribution, and the solid curves show the total fit.

B mass peak. As a consequence, it can be difficult to determine whether there are additional missing particles, especially neutrals. The neutrino and other missing particles degrade the B momentum resolution and hence reduce the precision of the proper decay time measurement. In addition, missing charged particles hinder the clean separation of B^0 and B^- samples. Figure 15 shows the proper time distributions from ALEPH⁷⁹ for $D^{*+}\ell^-$ and $D^0\ell^-$ samples, which would ideally correspond to \bar{B}^0 and B^- decays. In reality, the $D^{*+}\ell^-$ sample is $(87 \pm 4)\%$ pure, and the $D^0\ell^-$ is $(75 \pm 5)\%$ pure, so these distributions are fit simultaneously. A model is needed to account for possible feed-down contributions from various $D^{**}\ell^-\bar{\nu}$ modes. In spite of these complications, ALEPH achieves a very good systematic error on these measurements: $\tau_{B^0} = (1.61 \pm 0.07 \pm 0.04)$ ps and $\tau_{B^-} = (1.58 \pm 0.09 \pm 0.04)$ ps. DELPHI⁸⁰ reports a precise preliminary result $\tau(B^0) = (1.529 \pm 0.040 \pm 0.041)$ ps based on a study of $\bar{B}^0 \rightarrow D^{*+}X\ell^-\bar{\nu}$ decays. Their measurement is based on a novel method in which the D^0 from the $D^{*+} \rightarrow D^0\pi^+$ is inclusively reconstructed, leading to a sample of 3520 ± 150 decays.

The second method for determining b -hadron lifetimes uses fully reconstructed, exclu-

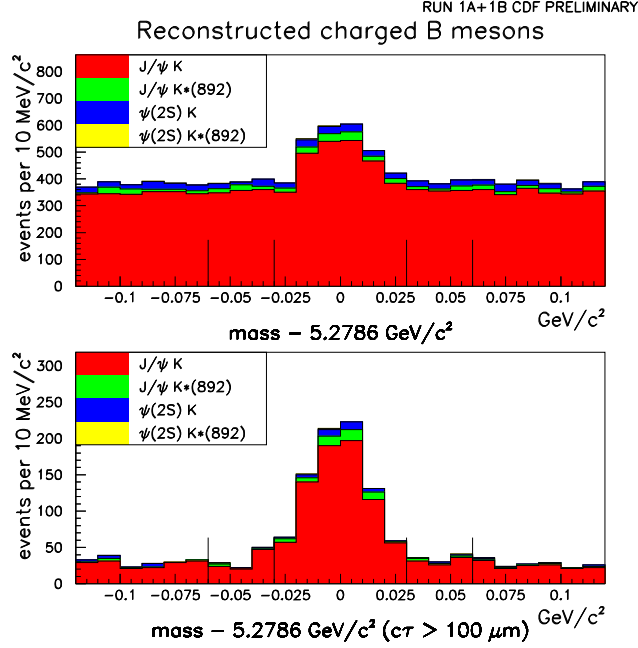


Figure 16: CDF measurement of $\tau(B^+)$. The upper histogram (a) shows the invariant mass distributions for B^+ candidates in the $J/\psi K^+$, $J/\psi K^{*+}$, $\psi(2S) K^+$ and $\psi(2S) K^{*+}$ final states; (b) shows the same distributions after the cut $c\tau > 100 \mu\text{m}$.

sive hadronic decays, and the analyses are usually much simpler than those using semileptonic modes. A b -hadron mass peak is observed, whose sidebands can be used to study the lifetime distribution of the background. Since all particles are observed, the decay vertex and the b hadron momentum are well determined, and the conversion to proper lifetime is very straightforward. The only disadvantage is that the event samples are typically smaller than those for semileptonic decay. In hadron colliders, however, a sufficiently large number of b hadrons is produced for exclusive hadronic decays to final states with J/ψ 's provide a competitive method for measuring lifetimes. Figure 16 shows the reconstructed B^+ mass from CDF⁸¹ for the final states $J/\psi K^+$, $J/\psi K^{*+}$, $\psi(2S) K^+$, and $\psi(2S) K^{*+}$. The upper and lower histogram in the figure show the data before and after the proper decay length cut $c\tau > 100 \mu\text{m}$. This cut is not actually used for the lifetime fit, but it demonstrates that the background is concentrated at short proper lifetimes. Figure 17 shows the distribution of proper decay lengths in the sig-

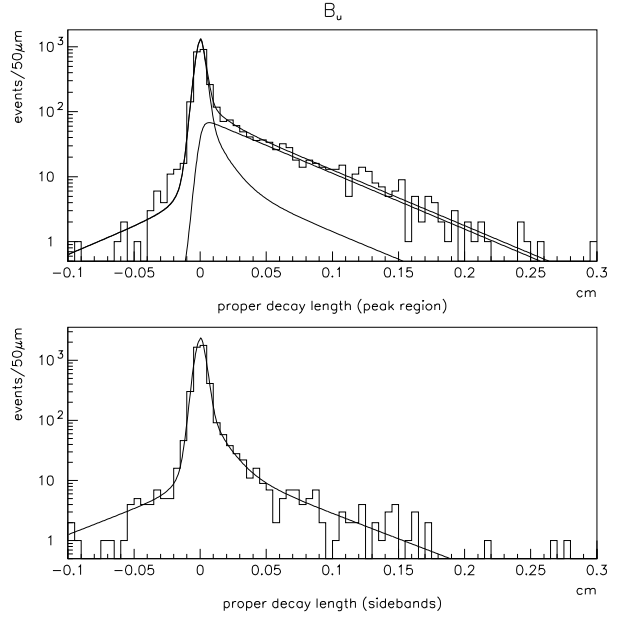


Figure 17: CDF measurement of $\tau(B^+)$. The upper histogram shows the proper decay length distribution for events in the B mass peak; the lower histogram shows the distribution for events in the B mass sidebands.

nal region (upper histogram) and in the B mass sidebands (lower histogram), together with the fits to the data. This measurement yields the value $\tau(B^+) = (1.68 \pm 0.07 \pm 0.02) \text{ ps}$, and a result of comparable precision is obtained for the B^0 lifetime.

The third method for measuring b hadron lifetimes makes use of topological vertexing, in which the B meson charge is determined from the total charge of the tracks associated with the decay vertex. Using this technique, SLD⁸² has obtained 6033 charged vertices and 3665 neutral vertices in a sample of only 150 thousand hadronic Z decays. Their measurement errors are comparable to those of many of the LEP and CDF results.

Figures 18 and 19 list the measured B^0 and B^- lifetimes and give the world averages computed by the LEP B Lifetime Working Group.⁸³ Their averages take into account the many sources of correlated experimental error, such as assumed fragmentation models, decay models, and branching fractions. To compare the B^0 and B^- lifetimes, it is best to calculate the lifetime ratio for each experiment, so that many systematics cancel,

and then to compute the average of the individual lifetime ratios. This average is

$$\tau(B^-)/\tau(B^0) = 1.04 \pm 0.04, \quad (17)$$

consistent with unity.

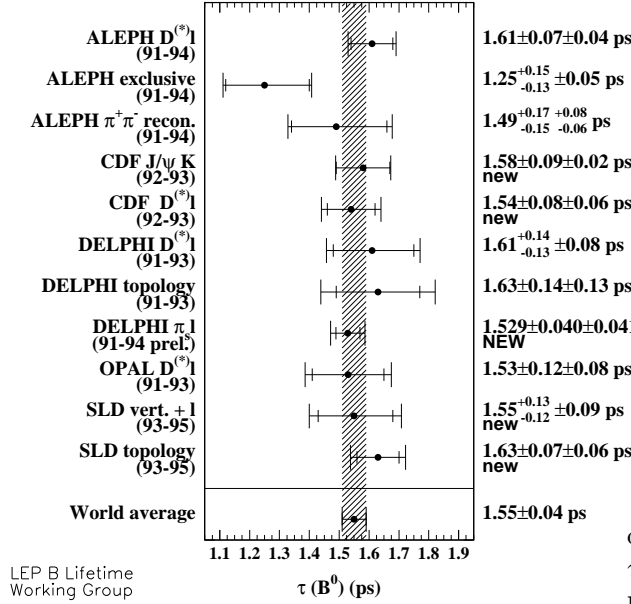


Figure 18: Summary of B^0 lifetime measurements.

Figure 20 summarizes measurements of the B_s lifetime. The uncertainties here are generally much larger than those for \bar{B}^0 and B^- lifetimes, due to smaller event samples and larger combinatorial backgrounds. Most of the measurements use the semileptonic decay $B_s \rightarrow D_s^+ X \ell^- \bar{\nu}$ and reconstruct the D_s^+ decay in one or more modes, although some use an inclusive D_s^+ signal or a D_s^+ with an associated hadron. The average lifetime from measurements based on these modes is $\tau(B_s) = 1.53 \pm 0.08$, consistent with the B^0 and B^- lifetimes.

Because the B_s^0 and \bar{B}_s^0 can oscillate into one another, the two mass eigenstates are expected to differ somewhat in their masses and lifetimes. Theoretical estimates indicate that the difference in decay widths may be as large as $\Delta\Gamma/\Gamma = 30\%$.⁸⁴ CDF⁸⁵ has reconstructed 58 ± 8 events in the decay $B_s \rightarrow J/\psi\phi$, which is expected to be predominantly CP even, in contrast to the $D_s^+\ell^-X$ final state, which is expected to be an equal mixture

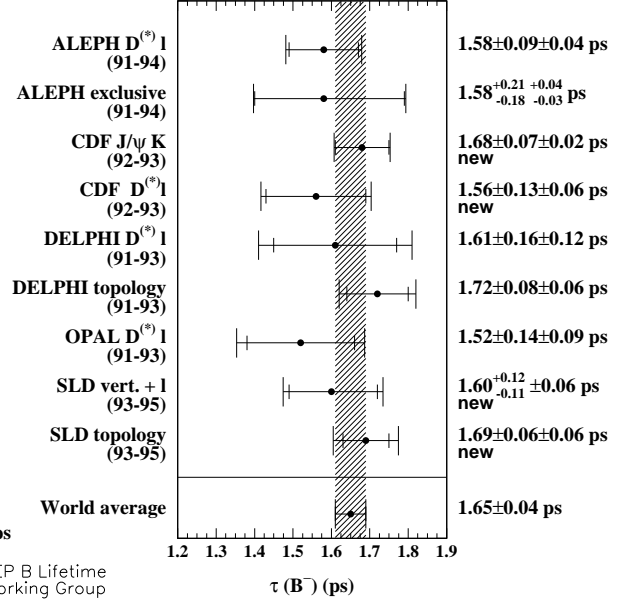


Figure 19: Summary of B^- lifetime measurements.

of CP even and CP odd. The preliminary result, $\tau(B_s) = 1.34^{+0.23}_{-0.19} \pm 0.05$ ps, is not yet sufficiently precise to address this issue, but future measurements with more data should be extremely interesting. More details on measurements of B^0 , B^- , and B_s lifetimes may be found in the talk of Claire Shepherd-Themistocleous.⁸⁶

The measured values of b -baryon lifetimes are systematically lower than those for B mesons. These analyses, which are described in more detail in the talk by Peter Ratoff⁸⁷, are performed using a variety of methods that select different compositions of b baryons, whose production fractions at the Z or at the Fermilab collider are not well known. (In fact, some papers use the symbol Λ_b to denote a generic b -baryon, but I use Λ_b^0 to denote the $I = 0$ *bud* ground state baryon.) Measurements of the Λ_b^0 lifetime generally use $\Lambda_c^\pm \ell^\mp$ correlations to select events from the decay $\Lambda_b^0 \rightarrow \Lambda_c^+ X \ell^- \bar{\nu}$. By fully reconstructing the $\Lambda_c^+ \rightarrow p K^- \pi^+$ decay and using kinematic cuts, one can obtain a high purity sample of $\Lambda_b^0 \rightarrow \Lambda_c^+ \ell^- \bar{\nu}$ decays. Alternatively, one can obtain larger event samples by using the inclusive decay $\Lambda_c^+ \rightarrow \Lambda X$ and searching for $\Lambda \ell^-$ or even $p \ell^-$ combinations. These methods, however,

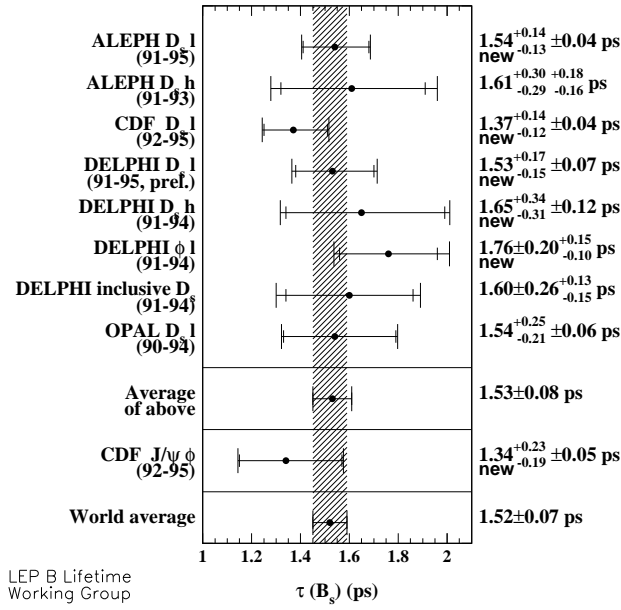


Figure 20: Summary of B_s lifetime measurements.

have a lower purity of Λ_b^0 baryons, since, for example, there can be background from $\Xi_b \rightarrow \Xi_c \ell^- \bar{\nu}$, $\Xi_c \rightarrow \Lambda X$.

Figure 21 shows the Λ_b^0 lifetime measurements obtained from $\Lambda_c^\pm \ell^\mp$ correlations in which the Λ_c^+ is fully reconstructed. The world average, $\tau_{\Lambda_b} = (1.23 \pm 0.09)$ ps, differs from the B^0 lifetime by about 3σ . By including measurements that use $\Lambda \ell^-$ and $p \ell^-$ correlations, the LEP B Lifetime Working Group obtains the average $\tau_{b\text{-baryon}} = (1.21 \pm 0.06)$ ps, or $\tau_{b\text{-baryon}}/\tau_{B^0} = 0.78 \pm 0.04$. This ratio is difficult to accommodate in calculations based on the $1/m_Q$ expansion, which predict a value in the range 0.9 to 1.0.

OPAL⁸⁸ has measured the ratio $R_{\Lambda\ell} = B(b\text{-baryon} \rightarrow \Lambda \ell X)/B(b\text{-baryon} \rightarrow \Lambda X)$, which should be a good approximation to the average b baryon semileptonic branching fraction. They obtain $R_{\Lambda\ell} = (6.8 \pm 1.3 \pm 1.0)\%$, which is consistent with the expectation based on the shorter b baryon lifetime and the assumption of equal semileptonic widths of B mesons and b baryons.

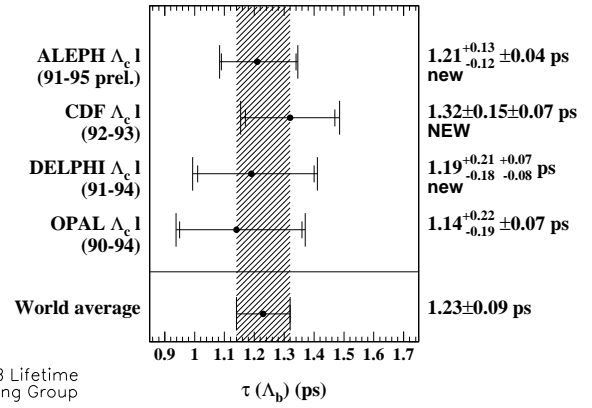


Figure 21: Summary of Λ_b lifetime measurements.

6 Conclusions

The combination of new measurements and new theoretical methods is transforming the subject of heavy-flavor dynamics. For many such processes, we have much more than a qualitative understanding: detailed, quantitative comparisons between theory and experiment have been performed, and the results are quite encouraging. In particular, there has been substantial progress on decay constants and semileptonic decay form factors. Quantities related to the hadronic rate, such as the inclusive semileptonic branching fraction, n_c , and b -hadron lifetimes, have proved to be more difficult to understand and have produced some intriguing puzzles. With the intensive effort underway at several laboratories, there is every reason to expect that these questions can be explored in great detail, and that many new ones will arise as rare decay modes become more accessible.

Acknowledgements

Many people contributed to this talk by providing plots, answering questions, and making suggestions on the presentation. I gratefully acknowledge the help of Thomas Browder, Andrzej Buras, John Carr, Lawrence Gibbons, I. Joseph Kroll, Guido Martinelli, Clara Matteuzzi, Ritchie Patterson, Peter Ratoff, Claire Shepherd-Themistocleous, Su Dong, and the LEP B -lifetimes working group. This work was supported by the U.S. Dept. of Energy grant DE-FG03-91ER40618.

References

1. L. Gibbons, 28th International Conference on High Energy Physics (ICHEP96), 25-31 July 1996, Warsaw, Poland, plenary session talk, these proceedings.
2. A. Buras, ICHEP96 plenary session talk, these proceedings.
3. G. Martinelli, ICHEP96 plenary session talk, these proceedings.
4. R. Landua, ICHEP96 plenary session talk, these proceedings.
5. J. D. Richman and P. R. Burchat, *Rev. Mod. Phys.* **67**, 893 (1995).
6. T. Browder, K. Honscheid, and D. Pedrini, University of Hawaii preprint UH-515-848-96, to be published in 1996 edition of *Annual Review of Nuclear and Particle Science*.
7. M. Neubert, *Phys. Rep.* **245**, 259 (1994).
8. A. Ali, hep-ph/9606324, DESY 96-106, to appear in Proceedings of XX International Nathiagali Summer College on Physics and Contemporary Needs, Bhurban, Pakistan, June 24–July 13, 1995.
9. I.I. Bigi, hep-ph 9507364, University of Notre Dame preprint UND-HEP-95-BIG06, in Proceedings of the 6th International Symposium on Heavy Flavor Physics, Pisa, Italy, June 6–10, 1995; hep-ph/9508408, UND-HEP-95-BIG02, to be published in *Physics Reports*.
10. M. Neubert, hep-ph/9604412, CERN-TH/96-55, to appear in *Intl. Journal of Mod. Phys. A*.
11. K. Kodama *et al.* (E653), hep-ex 9606017 (1996).
12. S. Aoki *et al.* (WA75), *Prog. Theor. Phys.* **89**, 131 (1993).
13. D. Gibaut *et al.* (CLEO), CLEO-CONF 95-22 (EPS-0184), submitted to the European Physical Society Conference, Brussels, Belgium (1995).
14. J.Z. Bai *et al.* (BES), *Phys. Rev. Lett.* **74**, 4599 (1995).
15. Review of Particle Properties, *Phys. Rev. D* **54**, Part I (1996).
16. C. Bernard *et al.* (MILC Collab.), WASH-U-HEP-96-31, hep-lat/9608092 (1996). Presented at Lattice 96: 14th International Symposium on Lattice Field Theory, St. Louis, MO, 4-8 Jun 1996.
17. A. Kunin, ICHEP96 parallel session talk, these proceedings.
18. D. Buskulic *et al.* *Phys. Lett. B* **343**, 444 (1995); see also ALEPH Collab., pa10-019, submitted to ICHEP96, Warsaw (1996).
19. J. Alexander *et al.* (CLEO), CLEO-CONF 94-5, submitted to the Intl. Conf. on High Energy Physics, Glasgow, Scotland (1994).
20. T.E. Browder *et al.* (CLEO), CLEO-CONF 96-14, ICHEP96 pa05-82 (1996).
21. N. Isgur and M.B. Wise, *Phys. Lett. B* **232**, 113 (1989).
22. N. Isgur and M.B. Wise, *Phys. Lett. B* **237**, 527 (1990).
23. F.E. Close and A. Wambach, *Phys. Lett. B* **348**, 207 (1995).
24. M.E. Luke, *Phys. Lett. B* **252**, 447 (1990).
25. T. Bergfeld *et al.* (CLEO), CLEO-CONF 96-3, ICHEP96 pa05-078 (1996).
26. ALEPH Collab., ICHEP96 pa05-056 (1996).
27. J.P. Alexander *et al.* (CLEO), CLEO-CONF 96-16, ICHEP96 pa05-81 (1996).
28. H. Albrecht *et al.* (ARGUS), *Phys. Lett. B* **229**, 175 (1989).
29. Review of Particle Properties, *Phys. Rev. D* **50**, Part I (1994).
30. J.E. Duboscq *et al.* (CLEO) *Phys. Rev. Lett.* **76**, 3898 (1996).
31. A. Anastassov *et al.* (CLEO), CLEO-CONF 96-8, ICHEP96 pa05-079 (1996).
32. D. Scora and N. Isgur, *Phys. Rev. D* **52**, 2783 (1995).
33. M. Neubert, *Phys. Lett. B* **338**, 84 (1994).
34. B. Barish *et al.* (CLEO), *Phys. Rev. D* **51**, 1014 (1995).
35. H. Albrecht *et al.* (ARGUS), *Z. Phys. C* **57**, 533 (1993).
36. P. Abreu *et al.*, (DELPHI), CERN-PPE/96-11, submitted to *Z. Phys. C* (1996).
37. OPAL Collab., ICHEP96 pa08-008 (1996).
38. I. Dunietz, hep-ph/9606247 (1996).
39. ALEPH Collab., ICHEP96 pa01-073 (1996).
40. T.E. Browder *et al.* (CLEO), CLEO-CONF 96-2, ICHEP96 pa05-77.
41. R. Akers *et al.* (OPAL), *Z. Phys. C* **67**, 57 (1995).
42. S. Anderson *et al.* (CLEO), CLEO-CONF 96-6, ICHEP96 pa05-080 (1996).
43. B. Barish *et al.* (CLEO), *Phys. Rev. Lett.* **76**, 1570 (1996).

44. H. Albrecht *et al.* (ARGUS), Phys. Lett.B **318**, 397 (1993).
45. ALEPH Collab., EPS-0404, contribution to the Int'l. Europhysics Conference on High Energy Physics, Brussels, Belgium (1995).
46. P. Abreu *et al.* (DELPHI), Z. Phys. C **66**, 323 (1995).
47. L3 Collab., CERN-PPE/96-49, submitted to Z. Phys. C (1996).
48. R. Akers *et al.* (OPAL), Z. Phys. C **60**, 199 (1993).
49. H. Albrecht *et al.* (ARGUS), Phys. Lett. B **324**, 249 (1994).
50. J.L. Rosner, in *B Decays*, edited by S. Stone (World Scientific, Singapore, 1992), p. 312.
51. A. Kagan, ICHEP96 parallel session talk, these proceedings.
52. I.I. Bigi, B. Blok, M. Shifman, and A. Vainshtein, Phys. Lett. B **323**, 408 (1994).
53. E. Bagan, P. Ball, B. Fiol, and P. Gosdzinsky, Phys. Lett. B **351**, 546 (1995).
54. E. Bagan, P. Ball, V.M. Braun, and P. Gosdzinsky, Phys. Lett. B **342**, 362 (1995); erratum-*ibid.* B **374**, 363 (1996).
55. M.B. Voloshin, Phys. Rev. D **51**, 3948 (1995).
56. ALEPH Collab., ICHEP pa05-061 (1996).
57. G. Alexander (OPAL), CERN-PPE/96-51, submitted to Z. Phys. C (1996).
58. G. Buchalla, I. Dunietz, and H. Yamamoto, FERMILAB-PUB-95/167-T, hep-ph/9507437 (1995).
59. ALEPH Collab., ICHEP Pa05-062 (1996).
60. P. Baringer *et al.* (HRS), Phys. Lett. B **206**, 551 (1988).
61. H. Albrecht *et al.* (ARGUS), Phys. Lett. B **340**, 125 (1995).
62. D.S. Akerib *et al.* (CLEO), Phys. Rev. Lett. **71**, 3070 (1993).
63. M. Artuso *et al.* (CLEO), Phys. Lett. B **378**, 364 (1996).
64. T. Browder, ICHEP96 parallel session talk, these proceedings.
65. J. Lewis, ICHEP96 parallel session talk, these proceedings.
66. T. Skwarnicki, ICHEP96 parallel session talk, these proceedings.
67. J.D. Bjorken, Nucl. Phys. B (Proc. Suppl.) **11**, 325 (1989).
68. M. Neubert, V. Rieckert, B. Stech, and Q.P. Xu, in *Heavy Flavors*, A.J. Buras and H. Linder, eds. (World Scientific, Singapore, 1992), p. 286.
69. D. Gibaut *et al.* (CLEO), Phys. Rev. D **53**, 4734 (1996).
70. M.S. Alam *et al.* (CLEO), Phys. Rev. D **50**, 43 (1994).
71. D.M. Asner *et al.* (CLEO), Phys. Rev. D **53**, 1039 (1996).
72. W. Adam *et al.* (DELPHI), CERN-PPE/96-67, submitted to Z. Phys. C (1996).
73. ALEPH Collab., ICHEP96 pa05-101 (1996).
74. B. Barish *et al.* CLEO-CONF 96-23, ICHEP96 pa05-095 (1996).
75. R. Ammar *et al.* (CLEO), CLEO-CONF 96-5, ICHEP96 pa05-93 (1996).
76. M. Artuso *et al.* (CLEO), CLEO-CONF 96-18, ICHEP96 pa05-73 (1996).
77. G. Brandenburg *et al.* (CLEO), CLEO-CONF 96-1, ICHEP96 pa05-96 (1996).
78. T. Bergfeld *et al.* (CLEO), CLEO-CONF 96-22, ICHEP96 pa05-92 (1996).
79. D. Buskulic *et al.* (ALEPH), CERN-PPE/96-14, submitted to Z. Phys. C (1996).
80. Delphi Collab., ICHEP96 pa1-041 (1996).
81. CDF,
<http://www-cdf.fnal.gov/physics/new/bottom/bottom.html> (1996).
82. SLD Collab., ICHEP96 PA05-085 (1996).
83. J. Alcaraz *et al.* (LEP *B* Lifetime Group),
<http://wwwcn.cern.ch/~claires/lepblife.html> (1996).
84. I. Dunietz, Phys. Rev. D **52**, 3048 (1996).
85. F. Abe *et al.* (CDF),
FERMILAB-PUB 96/101 E, submitted to Phys. Rev. Lett. (1996).
86. C. Shepherd-Themistocleous, ICHEP96 parallel session talk, these proceedings.
87. P. Ratoff, ICHEP96 parallel session talk, these proceedings.
88. OPAL Collab, ICHEP96 pa05-034 (1996).

Questions

Yung su Tsai, SLAC:

Will there ever be enough semileptonic decay events of B and D , so that we can measure the polarization of μ and τ ? If polarization is different for charged conjugate decay modes, it will indicate the non-standard model CP violation, i.e., the existence of a new charged gauge boson.

J. Richman:

It is not possible to measure the μ polarization, since these particles do not decay in the detector volume. In principle, one could measure the τ polarization in the decay $\bar{B} \rightarrow D^* \tau^- \bar{\nu}$, but it wouldn't be easy, and it would require a very large data sample. While this decay has been observed at LEP, it has not been seen at the $\Upsilon(4S)$, since the presence of two neutrinos (including the τ^- decay) makes its separation from background very difficult.

Bennie F. L. Ward, U. of Tennessee:

Could you explain why you say that the branching fraction $B(B \rightarrow D_s X)$ is experimentally different at CLEO and LEP, even though theoretically a particle's branching fraction to a given final state cannot depend on its velocity?

J. Richman:

This question is based on a misunderstanding. At LEP, the b -hadron mixture includes B_s mesons and b baryons in addition to B^+ and B^0 mesons. Measurements of D_s^+ production in this b -hadron mixture will therefore yield somewhat different results than measurements at the $\Upsilon(4S)$, where the b -hadron mixture includes only B^0 and B^+ .